Computational Challenges in Astrophysical Fluid Dynamics

ANDREA MIGNONE

DIPARTIMENTO DI FISICA
UNIVERSITÀ DI TORINO

Outline

1. ***Introduction***

2. ***Basic Discretization Methods for Hyperbolic PDE***:
   a. *Scalar advection equation*
   b. *Finite Volumes, Riemann Problem*
   c. *Systems of linear equations*
   d. *Nonlinear equation*
   e. *Extension to Euler Equations and MHD*
   f. *High-Order spatial and temporal accuracy;*

3. ***Applications to Astrophysical Problems:***
   a. *Accretion Disks*
   b. *Relativistic Jets*

1. Introduction

Observational Evidence

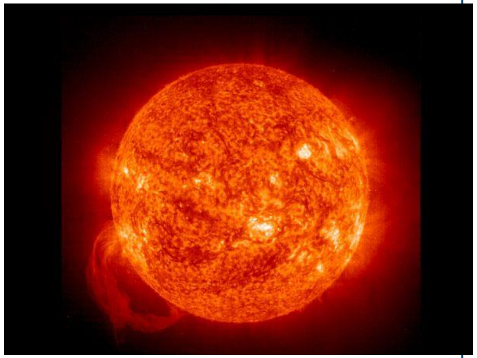

- It is estimated that more than 99.9 % of matter in the Universe exists in the form of *plasma*;
- A *plasma* is a ionized gas where charged particles interact via electromagnetic forces (electric and magnetic fields);
- Examples include stars, nebulae, galaxies, supernovae, interstellar/galactic medium, jets, accretion disks, etc..
- Our knowledge limited by what we can actually observe → *emitting plasma*.

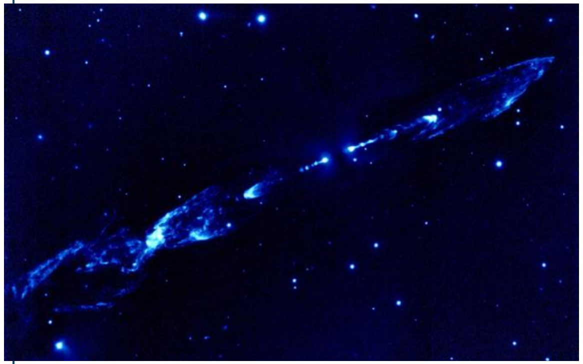

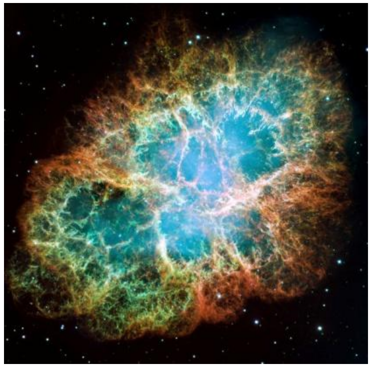

Astrophysical Plasma Conditions

- Astrophysical Plasmas are characterized by a wide disparity in spatial and temporal scales:

	L (cm)	n (cm^{-3})	T (K)	v(Km/s)	B (G)
Stellar interiors	$10^{10} \div 10^{12}$	10^{27}	$\geq 10^{7}$	$0 \div 500$	$1 \div 10^{4}$
Stellar winds	$10^{13} \div 10^{15}$	$10^{-2} \div 10^{3}$	$10^{2} \div 10^{3}$	$200 \div 4 \cdot 10^{3}$	$10^{-5} \div 10^{-3}$
Neutron star	10^{6}	10^{42}	$10^{6} \div 10^{9}$	-	10^{12}
Interstellar Medium	$10^{2} \div 10^{22}$	$10^{-1} \div 10$	10^{2}	$1 \div 30$	$\leq 10^{-5}$
Intergalactic Medium	$\geq 10^{24}$	$\leq 10^{-5}$	$10^{5} \div 10^{6}$	$10 \div 10^{3}$	$\leq 10^{-8}$
Jets from YSO	$10^{16} \div 10^{18}$	$10^{3} \div 10^{4}$	$10^{3} \div 10^{5}$	$100 \div 500$	$10^{-4} \div 10^{-3}$
Jets in AGN	$10^{21} \div 10^{24}$	$10^{-5} \div 10^{-3}$	-	$\sim c$	$\sim 10^{-3}$

- Flows are compressible, magnetized, supersonic, and possibly relativistic;
- Several physical effects: advection, dissipative (non-ideal effects), cooling/radiation, gravity, non-inertial effects, complex equations of state, stiff reaction networks, etc…

Plasma Description

- Most theoretical models are based on a fluid description ($L \gg \lambda_{mfp}$) requiring the solution of highly nonlinear hyperbolic / parabolic P.D.E., e.g.

Euler equations

$$\begin{aligned}
\frac{\partial \rho}{\partial t} + \nabla \cdot (\rho \boldsymbol{v}) &= 0 \\
\frac{\partial (\rho \boldsymbol{v})}{\partial t} + \nabla \cdot \left(\rho \boldsymbol{v}\boldsymbol{v}^T\right) + \nabla p &= \rho \boldsymbol{a} + \nabla \cdot \Pi \\
\frac{\partial E}{\partial t} + \nabla \cdot [(E+p)\,\boldsymbol{v}] &= \rho \boldsymbol{v} \cdot \boldsymbol{a} + \nabla \cdot (\boldsymbol{v} \cdot \Pi) + \nabla \cdot \boldsymbol{F}_c
\end{aligned}$$

Single Fluid MHD equations

$$\begin{aligned}
\frac{\partial \rho}{\partial t} + \nabla \cdot (\rho \boldsymbol{v}) &= 0 \\
\frac{\partial (\rho \boldsymbol{v})}{\partial t} + \nabla \cdot \left[\rho \boldsymbol{v}\boldsymbol{v}^T - \boldsymbol{B}\boldsymbol{B}^T\right] + \nabla \left(p + \frac{\boldsymbol{B}^2}{2}\right) &= \rho \boldsymbol{a} + \nabla \cdot \Pi \\
\frac{\partial \boldsymbol{B}}{\partial t} - \nabla \times (\boldsymbol{v} \times \boldsymbol{B}) &= -\nabla \times (\eta \boldsymbol{J}) \\
\frac{\partial E}{\partial t} + \nabla \cdot [(E+p_T)\,\boldsymbol{v} - (\boldsymbol{B} \cdot \boldsymbol{v})\,\boldsymbol{B}] &= \rho \boldsymbol{v} \cdot \boldsymbol{a} - \nabla \cdot (\eta \boldsymbol{J} \times \boldsymbol{B}) + \nabla \cdot (\boldsymbol{v} \cdot \Pi) + \nabla \cdot \boldsymbol{F}_c
\end{aligned}$$

Why numerical simulations ?

- Exact solutions possible under very restrictive assumptions, e.g. stationarity ($\partial/\partial t = 0$), self-similarity, spherically symmetry or similar.

- Nonlinear, time-dependent systems can be studied only by means of numerical simulations.

- Grid-Based fluid approach via Finite Volume/Difference:
  - Fluid variables are discretized on a spatial grid (static or adaptive) and evolved in time.
  - Numerical solution of hyperbolic PDE in presence of discontinuous waves
  - Shock-Capturing (or Godunov-type) schemes.

A computational example:
Rayleigh-Taylor unstable flows

- ***Problem:***

  Supernova remnants morphology & Rayleigh Taylor Instability

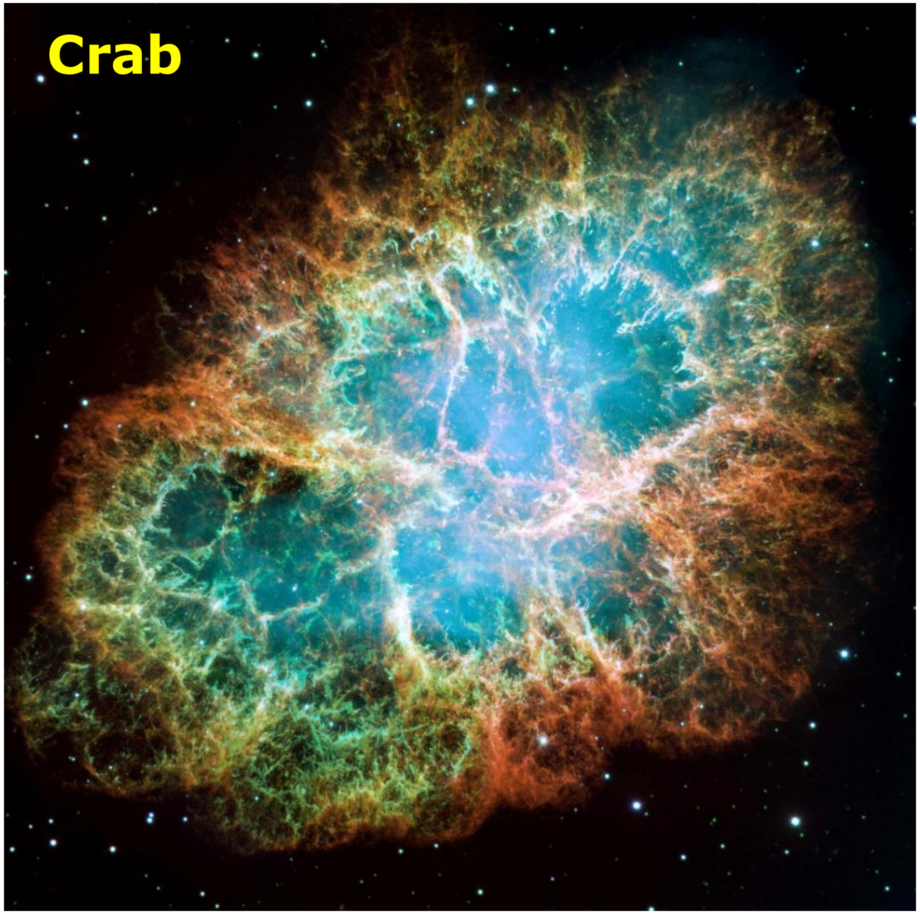

A computational example:
Rayleigh-Taylor unstable flows

- ***Problem:***

  Supernova remnants morphology & Rayleigh Taylor Instability

- Choose computational domain

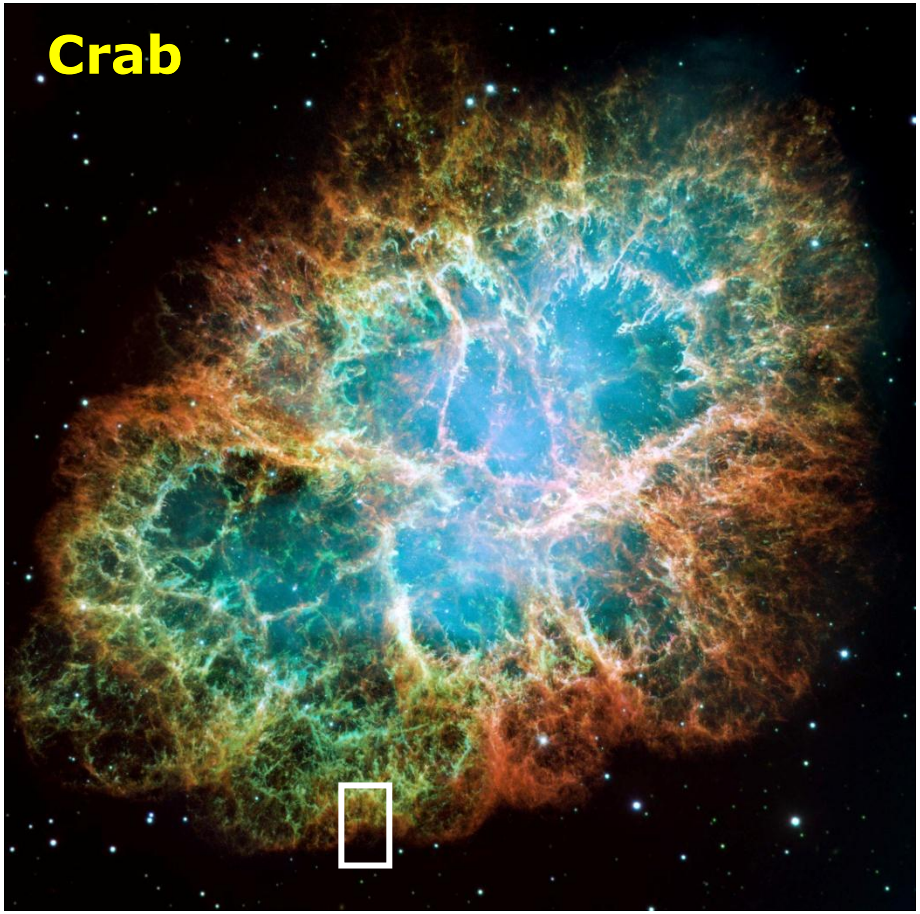

A computational example:
Rayleigh-Taylor unstable flows

- ***Problem:***

  Supernova remnants morphology & Rayleigh Taylor Instability

- Choose computational domain
- Set the number of zones

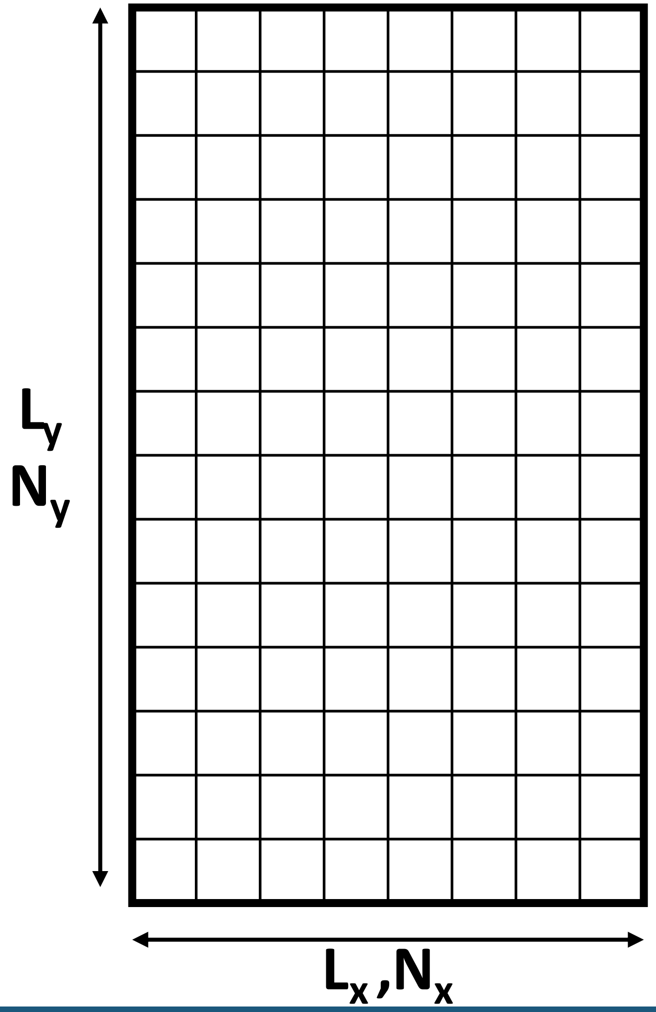

A computational example:

Rayleigh-Taylor unstable flows

- ***Problem:***

  Supernova remnants morphology & Rayleigh Taylor Instability

- Choose computational domain
- Set the number of zones
- Set initial conditions:

$$\rho = \begin{cases} 2 & \text{for} \quad y > 0 \\ 1 & \text{for} \quad y < 0 \end{cases} \qquad p = \frac{1}{\gamma} - \rho g y\,, \quad v_x = 0\,, \quad v_y = \epsilon R \left[1 + \cos\left(\frac{2\pi y}{L_y}\right)\right]$$

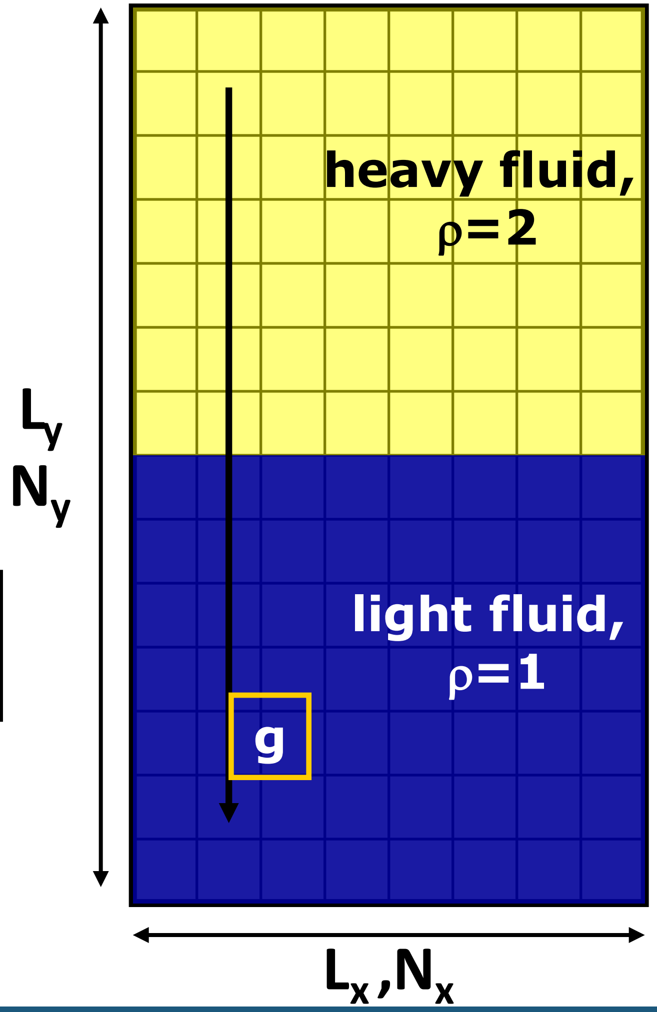

A computational example:
Rayleigh-Taylor unstable flows

- ***Problem:***

  Supernova remnants morphology & Rayleigh Taylor Instability

- Choose computational domain
- Set the number of zones
- Set initial conditions:

$$\rho = \begin{cases} 2 & \text{for} \quad y > 0 \\ 1 & \text{for} \quad y < 0 \end{cases} \qquad p = \frac{1}{\gamma} - \rho g y\,, \quad v_x = 0\,, \quad v_y = \epsilon R\left[1 + \cos\left(\frac{2\pi y}{L_y}\right)\right]$$

- Set boundary conditions

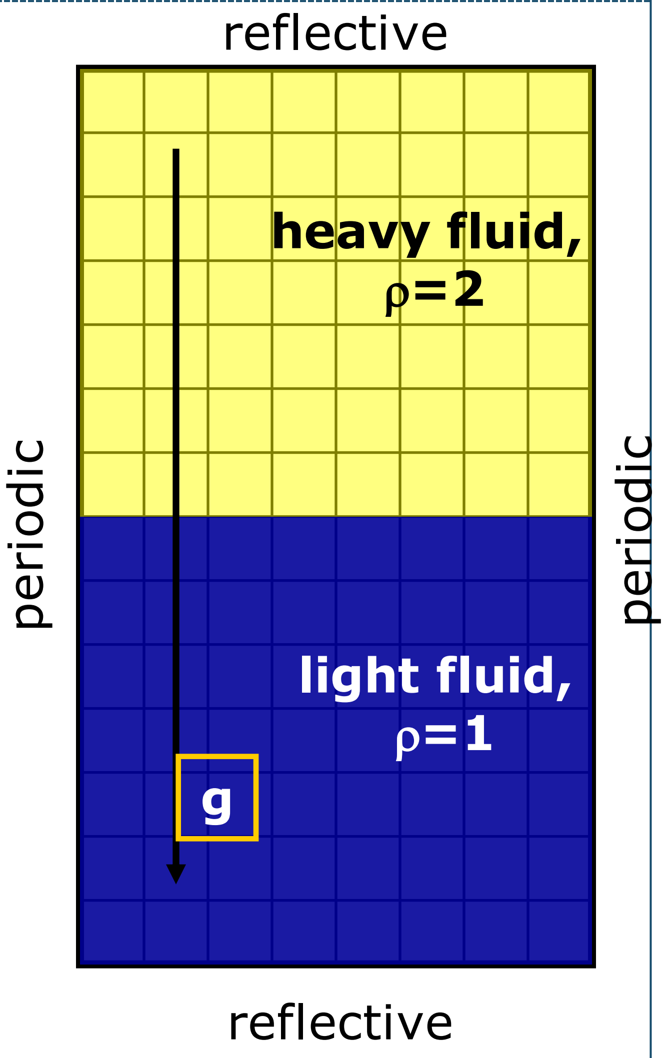

A computational example:
Rayleigh-Taylor unstable flows

- ***Problem:***

  Supernova remnants morphology & Rayleigh Taylor Instability

- Choose computational domain
- Set the number of zones
- Set initial conditions:

$$\rho = \begin{cases} 2 & \text{for} \quad y > 0 \\ 1 & \text{for} \quad y < 0 \end{cases} \qquad p = \frac{1}{\gamma} - \rho g y\,, \quad v_x = 0\,, \quad v_y = \epsilon R\left[1 + \cos\left(\frac{2\pi y}{L_y}\right)\right]$$

- Set boundary conditions
- Set final integration time & Run!

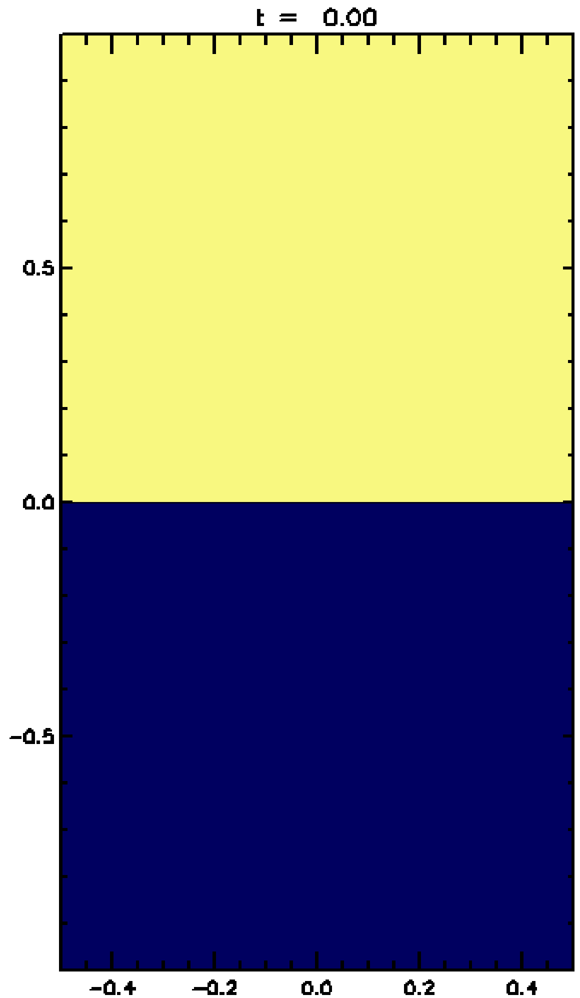

2a. Basic discretization for hyperbolic PDE: Linear advection Equation

The Advection Equation: Theory

- First order partial differential equation (PDE) in (x,t):

$$\frac{\partial q(x,t)}{\partial t} + a\frac{\partial q(x,t)}{\partial x} = 0$$

- Hyperbolic PDE: information propagates across domain at finite speed → method of characteristics
- Characteristic curves are the solutions of the equation

$$\frac{dx}{dt} = a$$

- So that, along each characteristic, the solution satisfies

$$\frac{dq}{dt} = \frac{\partial q}{\partial t} + \frac{dx}{dt}\frac{\partial q}{\partial x} = 0$$

The Advection Equation: Theory

- The solution is constant along the characteristic curves. At any point (x,t) we trace the characteristic back to the initial position.

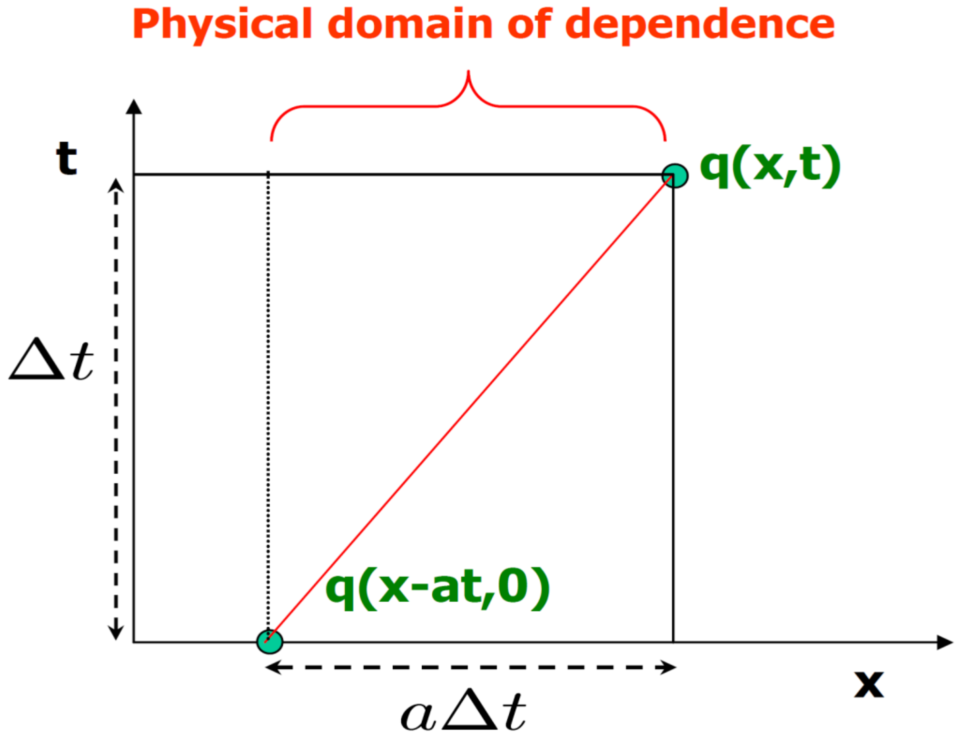

- This defines the physical domain of dependence.

The Advection Equation: Theory

- for constant *a*: the characteristics are straight parallel lines and the solution to the PDE is a uniform shift of the initial profile:

$$q(x,t) = \phi(x - at)$$

- Here $\phi(x) = q(x,0)$ is the initial condition

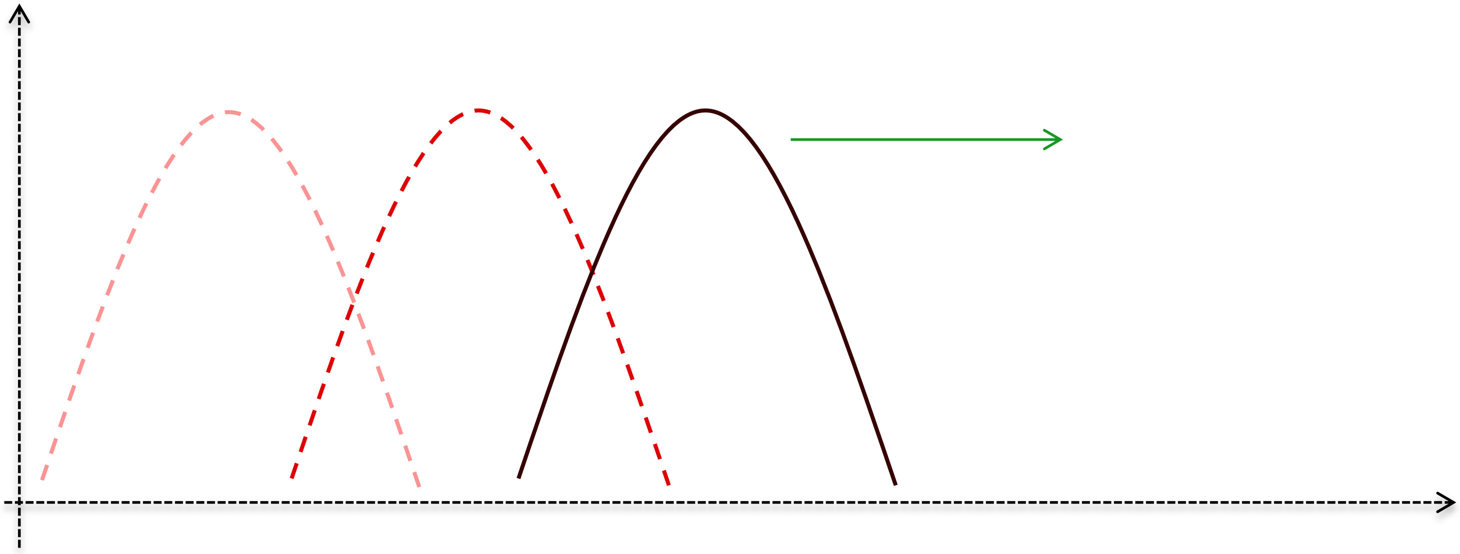

Numerical Discretizations

$$\frac{\partial q}{\partial t} + a\frac{\partial q}{\partial x} = 0$$

- Two popular methods for performing discretization:

  - *Finite Differences* (FD);
  - *Finite Volume* (FV);

- For some problems, the resulting discretizations look identical, but they are distinct approaches;
- We begin using finite-difference as it will allow to quickly learn some important concepts.

Finite Difference Approach

- A finite-difference method stores the solution at specific points in space and time;

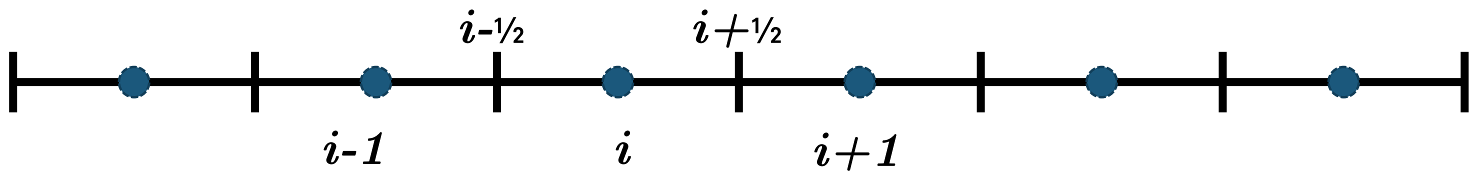

- Associated with each grid point is a function value,

$$q_i^n = q(x_i, t^n)$$

- We replace the derivatives in our PDE with differences between neighbor points

Finite Volume Approach

- In a finite volume discretization, the unknowns are the spatial averages of the function itself:

$$\langle q \rangle_i^n = \frac{1}{\Delta x} \int_{x_{i-\frac{1}{2}}}^{x_{i+\frac{1}{2}}} q(x, t^n)\, dx$$

where i-½ and i-½ denote the location of the interfaces.

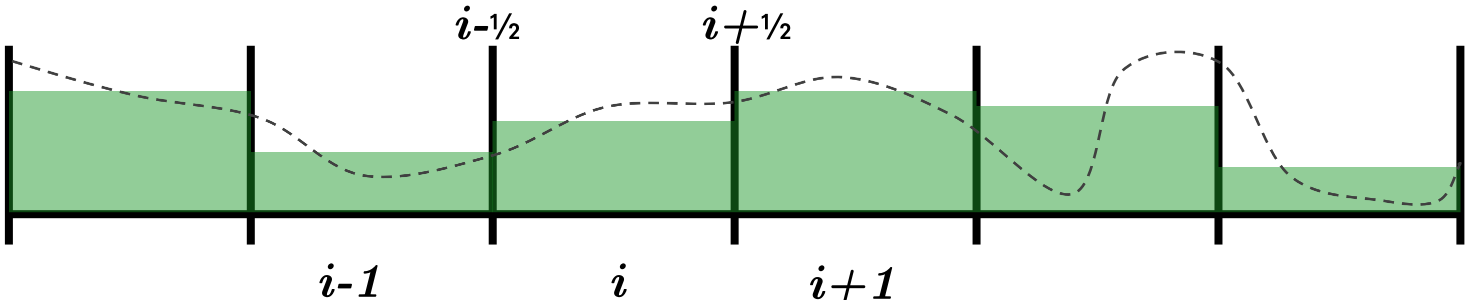

- The solution to the conservation law involves computing fluxes through the boundary of the control volumes

Discretization: the FTCS scheme

- We need to approximate the derivatives in our PDE

$$\frac{\partial q(x,t)}{\partial t} + a\frac{\partial q(x,t)}{\partial x} = 0$$

- In time, use forward derivative, since we want to use information from the previous time level

$$\frac{\partial q(x,t)}{\partial t} \approx \frac{q_i^{n+1} - q_i^n}{\Delta t} + O(\Delta t)$$

- In space, we use centered derivatives, since it is more accurate:

$$\frac{\partial q(x,t)}{\partial x} \approx \frac{q_{i+1}^n - q_{i-1}^n}{2\Delta x} + O(\Delta x^2)$$

The FTCS scheme

- Putting all together: $$\frac{q_i^{n+1} - q_i^n}{\Delta t} + a\left(\frac{q_{i+1}^n - q_{i-1}^n}{2\Delta x}\right) = 0$$
- and solving with respect to q_i^{n+1} gives

$$q_i^{n+1} = q_i^n - \frac{C}{2}\left(q_{i+1}^n - q_{i-1}^n\right)$$

where $C = a\dfrac{\Delta t}{\Delta x}$ is the Courant-Friedrichs-Lewy (CFL) number

- We call this method *FTCS* for forward in time, centered in space.
- The value at the new time level depends only on quantities at the previous time steps → *explicit* method

The FTCS scheme

- At t=0, the ***initial condition*** is a square pulse with periodic boundary conditions:

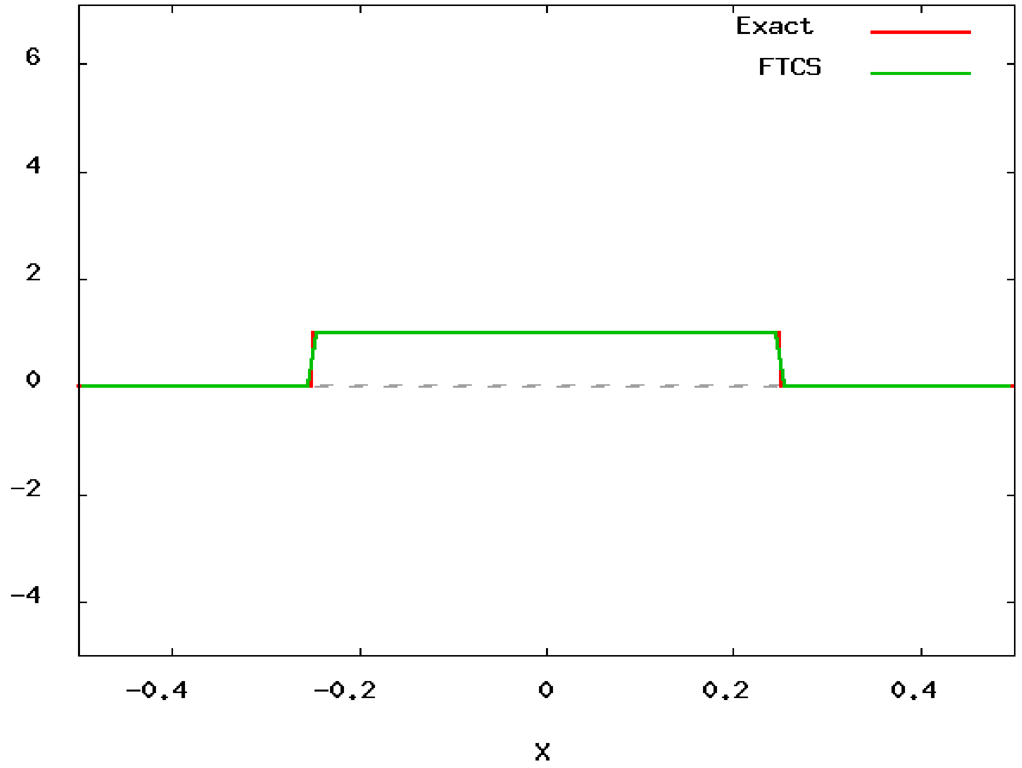

The FTCS scheme

- After some time, the solution looks like this:

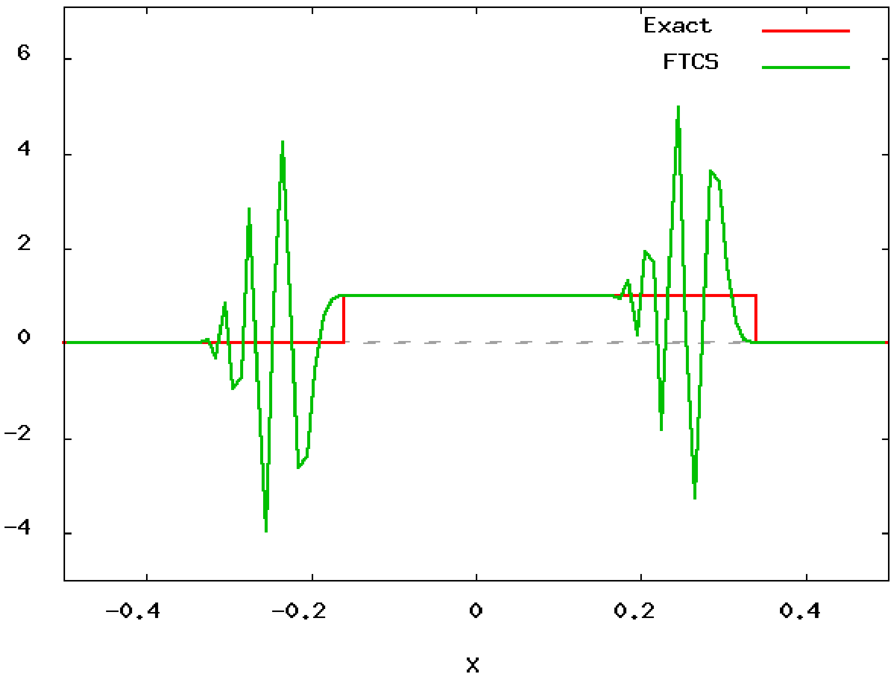

- Something isn't right… why ?

von Neumann Stability Analysis

- Let's perform an analysis of *FTCS* by expressing the solution as a Fourier series.

- Since the equation is linear, we only examine the behavior of a single mode. Consider a trial solution of the form

$$q_i^n = A^n e^{Ii\theta}, \quad \theta = k\Delta x$$

- This is a spatial Fourier expansion. Plugging in the difference formula:

$$q_i^{n+1} = q_i^n - \frac{C}{2}\left(q_{i+1}^n - q_{i-1}^n\right) \implies A^{n+1} = A^n - \frac{C}{2}A^n\left(e^{I\theta} - e^{-I\theta}\right)$$

von Neumann Stability Analysis

- Defining the amplification factor $\dfrac{A^{n+1}}{A^n}$ one obtains

$$\frac{A^{n+1}}{A^n} = 1 - \frac{C}{2}\left(e^{I\theta} - e^{-I\theta}\right) = 1 - IC\sin\theta$$

- a method is well-behaved or stable when $\left|\dfrac{A^{n+1}}{A^n}\right| \leq 1$
- however, for FTCS, one gets $\left|\dfrac{A^{n+1}}{A^n}\right|^2 = 1 + C^2\sin^2\theta \geq 1$
- Indipendently of the CFL number, all Fourier modes increase in magnitude as time advances
- This method is unconditionally unstable!

Forward in time, backward in space

- Let's use a difference approach. Consider the backward formula for the spatial derivative:

$$\frac{\partial q(x,t)}{\partial x} \approx \frac{q_i^n - q_{i-1}^n}{\Delta x} + O(\Delta x)$$

- Apply von Neumann stability analysis on the resulting discretized equation:

$$\frac{q_i^{n+1} - q_i^n}{\Delta t} + a\left(\frac{q_i^n - q_{i-1}^n}{\Delta x}\right) = 0$$

- Solving for the amplification factor gives

$$\left|\frac{A^{n+1}}{A^n}\right|^2 = 1 - 2C(1-C)(1-\cos\theta)$$

Forward in time, backward in space

- The method is stable when $\left|\frac{A^{n+1}}{A^n}\right| \leq 1 \rightarrow 2C(1-C) \geq 0$
- for a < 0 the method is *unstable*, but
- for a > 0 the method is stable when $0 \leq a\frac{\Delta t}{\Delta x} \leq 1$

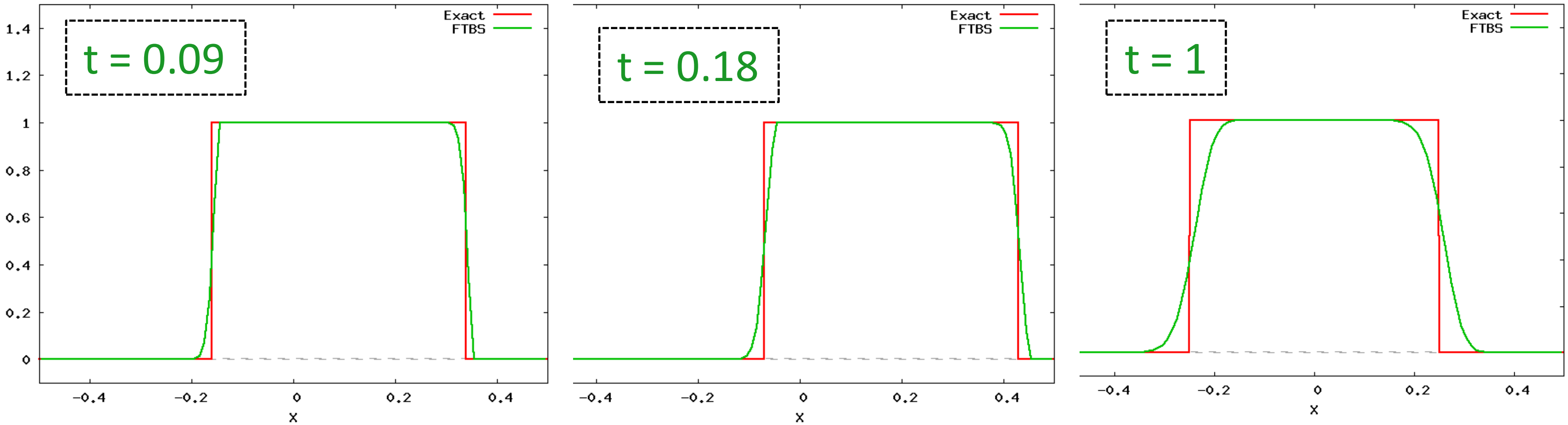

Forward in time, forward in space

- Repeating the same argument for the forward derivative

$$\frac{q_i^{n+1} - q_i^n}{\Delta t} + a\left(\frac{q_{i+1}^n - q_i^n}{\Delta x}\right) = 0$$

- Gives $$\left|\frac{A^{n+1}}{A^n}\right|^2 = 1 + 2C(1+C)(1-\cos\theta)$$

- If *a > 0* the method will always be <u>unstable</u>

- However, if $-1 \leq a\frac{\Delta t}{\Delta x} \leq 0$, then this method is <u>stable</u>;

The CFL condition

- Since the advection speed *a* is a parameter of the equation, Δx is fixed from the grid, the previous inequality is a stability constraint on the time step

$$\Delta t \leq \frac{\Delta x}{|a|}$$

- Δt cannot be arbitrarily large but, rather, less than the time taken to travel one grid cell (CFL condition).

- In the case of nonlinear equations, the speed can vary in the domain and the maximum of *a* should be considered instead.

The first-order Godunov Method

- Summarizing: the stable discretization makes use of the grid point where information is coming from:

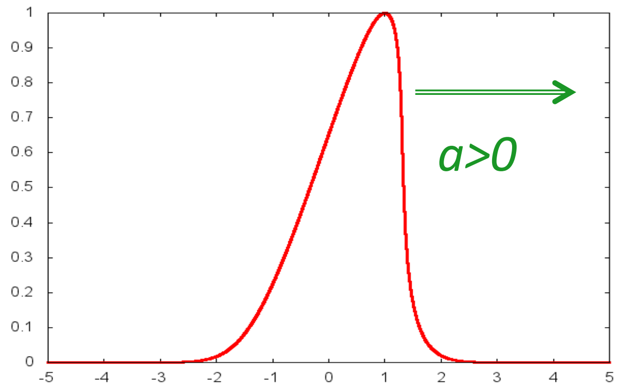

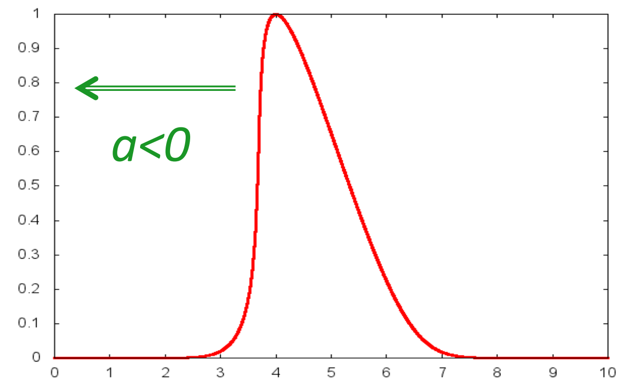

- This is *"upwind"*:

$$\begin{cases} q_i^{n+1} = q_i^n - \dfrac{a\Delta t}{\Delta x}\left(q_i^n - q_{i-1}^n\right) & \text{for} \quad a > 0 \\ q_i^{n+1} = q_i^n - \dfrac{a\Delta t}{\Delta x}\left(q_{i+1}^n - q_i^n\right) & \text{for} \quad a < 0 \end{cases}$$

- This is also called the first-order Godunov method;

Conservative Form

- We define the "flux" function $F^n_{i+\frac{1}{2}} = \frac{a}{2}\left(q^n_{i+1} + q^n_i\right) - \frac{|a|}{2}\left(q^n_{i+1} - q^n_i\right)$
- so that Godunov method can be cast in conservation form

$$q_i^{n+1} = q_i^n - \frac{\Delta t}{\Delta x}\left(F^n_{i+\frac{1}{2}} - F^n_{i-\frac{1}{2}}\right)$$

a > 0

$$q_i^{n+1} = q_i^n - \frac{a\Delta t}{\Delta x}\left(q_i^n - q_{i-1}^n\right)$$

a < 0

$$q_i^{n+1} = q_i^n - \frac{a\Delta t}{\Delta x}\left(q_{i+1}^n - q_i^n\right)$$

- The conservative form ensures a correct description of *discontinuities* in nonlinear system, ensures global *conservation* properties and is the main building block in the development of high-order *finite volume* schemes.

2b. Basic discretization for hyperbolic PDE: Finite Volume & Riemann Problem

Finite Volume Formulation

- The *conservative form* of the equations provides the link between the *differential* form of the equation,

$$\frac{\partial \boldsymbol{q}}{\partial t} + \frac{\partial \boldsymbol{F}}{\partial t} = 0$$

and the *integral* form, obtained by integrating the equations over a time interval $\Delta t = t^{n+1} - t^{n}$ and cell size $\Delta x = x_{i+1/2} - x_{i-1/2}$

$$\int_{t^n}^{t^{n+1}} \int_{x_{i-\frac{1}{2}}}^{x_{i+\frac{1}{2}}} \left(\frac{\partial \boldsymbol{q}}{\partial t} + \frac{\partial \boldsymbol{F}}{\partial x} \right) dt\, dx$$

Finite Volume Formulation

- Performing the spatial integration yields

$$\int_{t^n}^{t^{n+1}} \left[\Delta x \frac{d}{dt} \langle \boldsymbol{q} \rangle_i + \left(\boldsymbol{F}_{i+\frac{1}{2}} - \boldsymbol{F}_{i-\frac{1}{2}} \right) \right] dt = 0$$

with $\langle \boldsymbol{q} \rangle_i = \frac{1}{\Delta x} \int_{x_{i-\frac{1}{2}}}^{x_{i+\frac{1}{2}}} \boldsymbol{q}(x,t)\, dx$ being a *spatial* average.

- A second integration in time gives

$$\Delta x \left(\langle \boldsymbol{q} \rangle_i^{n+1} - \langle \boldsymbol{q} \rangle_i^{n} \right) + \Delta t \left(\tilde{\boldsymbol{F}}^n_{i+\frac{1}{2}} - \tilde{\boldsymbol{F}}^n_{i-\frac{1}{2}} \right) = 0$$

where $\tilde{\boldsymbol{F}}^n_{i\pm\frac{1}{2}} = \frac{1}{\Delta t} \int_{t^n}^{t^{n+1}} \boldsymbol{F}\left(\boldsymbol{q}(x_{i\pm\frac{1}{2}}, t) \right) dt$ is a *temporal* average

Finite Volume Formulation

- Rearranging terms yields

$$\langle \boldsymbol{q} \rangle_i^{n+1} = \langle \boldsymbol{q} \rangle_i^n - \frac{\Delta t}{\Delta x} \left(\tilde{\boldsymbol{F}}_{i+\frac{1}{2}}^n - \tilde{\boldsymbol{F}}_{i-\frac{1}{2}}^n \right)$$

Integral form

with spatial and temporal averages given by

$$\langle \boldsymbol{q} \rangle_i = \frac{1}{\Delta x} \int_{x_{i-\frac{1}{2}}}^{x_{i+\frac{1}{2}}} \boldsymbol{q}(x,t)\, dx \qquad \tilde{\boldsymbol{F}}_{i\pm\frac{1}{2}}^n = \frac{1}{\Delta t} \int_{t^n}^{t^{n+1}} \boldsymbol{F}\Big(\boldsymbol{q}(x_{i\pm\frac{1}{2}}, t) \Big)\, dt$$

- We have derived an *EXACT* evolutionary equation for the spatial averages of *q*.
- This relation provides an *integral* representation of the original differential equation.
- The integral form does not make use of partial derivatives!

The Riemann Problem

- The previous relations are exact.
- However, since the solution is known only at t^n, some kind of approximation is required in order to evaluate the flux through the boundary:

$$\tilde{\boldsymbol{F}}^n_{i\pm\frac{1}{2}} = \frac{1}{\Delta t}\int_{t^n}^{t^{n+1}} \boldsymbol{F}\Big(\boldsymbol{q}(x_{i\pm\frac{1}{2}}, t)\Big)\, dt$$

- This achieved by solving the so-called "*Riemann Problem*", i.e., the evolution of an inital discontinuity separating two constant states. The Riemann problem is defined by the initial condition:

$$\boldsymbol{q}(x,0) = \begin{cases} \boldsymbol{q}_L & \text{for} \quad x < x_{i+\frac{1}{2}} \\ \boldsymbol{q}_R & \text{for} \quad x > x_{i+\frac{1}{2}} \end{cases} \quad \Longrightarrow \quad \boldsymbol{q}(x_{i+\frac{1}{2}}, t) = ??$$

The Riemann Problem

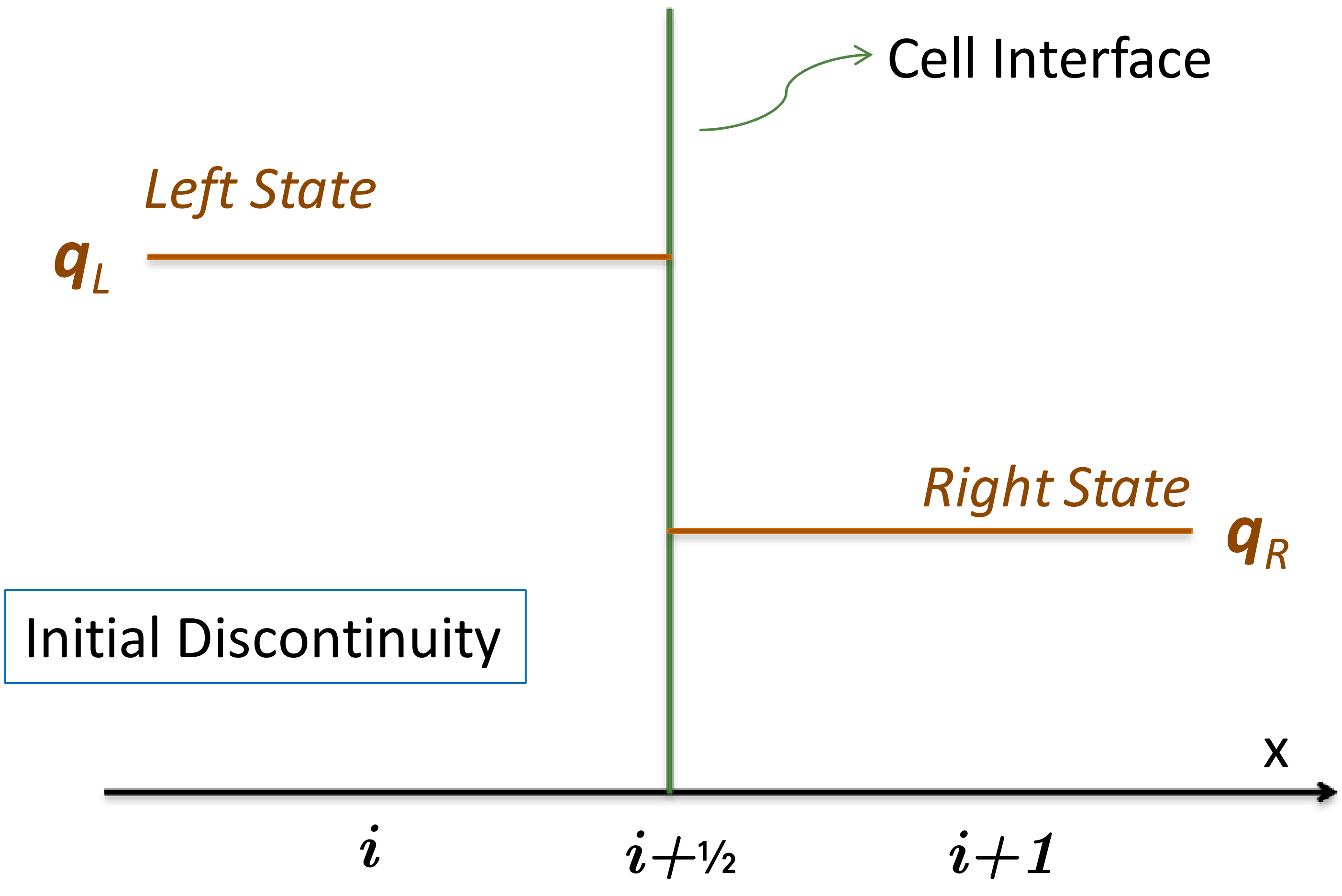

The Riemann Problem

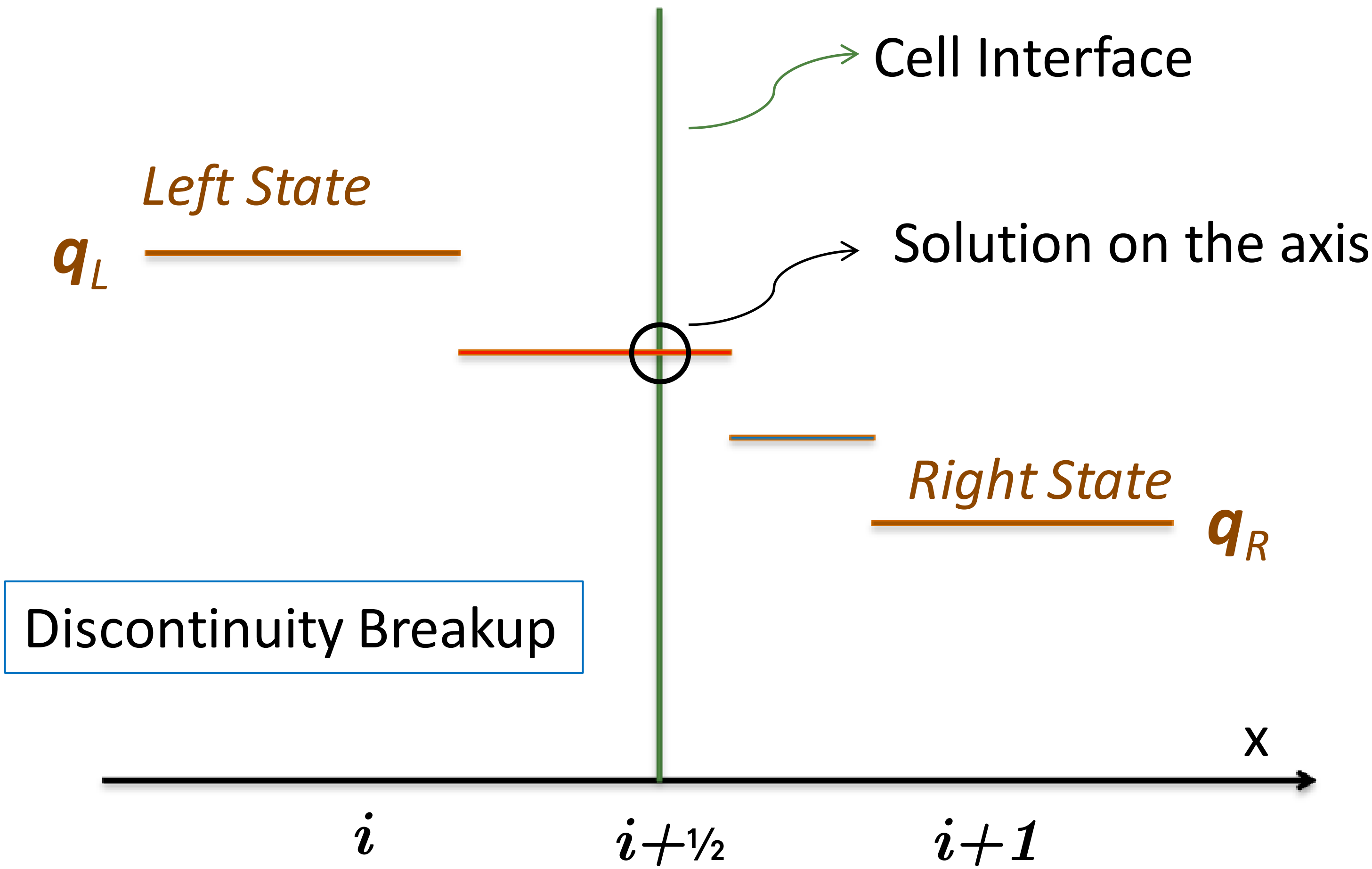

2c. Basic discretization for hyperbolic PDE: Systems of Linear Equations

System of Equations: theory

- We turn our attention to the system of equations (PDE)

$$\frac{\partial \mathbf{q}}{\partial t} + A \cdot \frac{\partial \mathbf{q}}{\partial x} = 0$$

where $\mathbf{q} = \{q_1, q_2, \dots q_m\}$ is the vector of unknowns. A is a m x m constant matrix.

- The system is hyperbolic if A has real eigenvalues, $\lambda^1 \leq \dots \leq \lambda^m$ and a complete set of linearly independent right and left eigenvectors $\boldsymbol{r}^k$ and $\boldsymbol{l}^k$ ($\boldsymbol{r}^j \cdot \boldsymbol{l}^k = \delta_{jk}$) such that

$$\begin{cases} A \cdot \boldsymbol{r}^k = \lambda^k \boldsymbol{r}^k \\ \boldsymbol{l}^k \cdot A = \boldsymbol{l}^k \lambda^k \end{cases} \quad \text{for} \quad k = 1, \dots, m$$

System of Equations: theory

- In this form, the system decouples into *m* independent advection equations for the characteristic variables:

$$\frac{\partial \boldsymbol{w}}{\partial t} + \Lambda \cdot \frac{\partial \boldsymbol{w}}{\partial x} = 0 \quad \Longrightarrow \quad \frac{\partial w^k}{\partial t} + \lambda^k \cdot \frac{\partial w^k}{\partial x} = 0$$

where $w^k = \mathbf{l}^k \cdot \mathbf{q}$ (k=1,2,…,m) is a characteristic variable.

- Each equations has the *exact analytical solution*

$$w^k(x,t) = w^k(x - \lambda^k t, 0)$$

i.e., the initial profile of w^k "shifts" with uniform velocity λ^k

System of Equations: Exact Solution

- Once the solutions in characteristic form are known, we can solve the original system via the inverse transformation

$$\mathbf{q}(x,t) = \sum_{k=1}^{k=m} \mathbf{l}^k \cdot \mathbf{q}(x - \lambda^k t, 0)\mathbf{r}^k$$

- The characteristic variables are thus the coefficients of the right eigenvector expansion of q.

- The solution to the linear system reduces to a linear combination of m linear waves traveling with velocities λ^k .

System of Equations: Numerics

- We suppose the solution at time level *n* is known as q^n and we wish to compute the solution q^{n+1} at the next time level *n+1*.

- Our numerical scheme can be derived by working in the characteristic space and then transforming back:

$$\boldsymbol{q}_i^{n+1} = \sum_k w_i^{k,n+1} \boldsymbol{r}^k = \boldsymbol{q}_i^n - \frac{\Delta t}{\Delta x}\left(\boldsymbol{F}^n_{i+\frac{1}{2}} - \boldsymbol{F}^n_{i-\frac{1}{2}}\right)$$

where $$\boldsymbol{F}^n_{i+\frac{1}{2}} = A \cdot \frac{\boldsymbol{q}^n_{i+1} + \boldsymbol{q}^n_i}{2} - \frac{1}{2}\sum_k |\lambda^k| \boldsymbol{l}^k \cdot (\boldsymbol{q}^n_{i+1} - \boldsymbol{q}^n_i)\boldsymbol{r}^k$$

is the *Godunov flux* for a linear system of advection equations.

The Riemann Problem

- If $\boldsymbol{q}$ is initially discontinuous, one or more characteristic variables will also have a discontinuity. Indeed, at $t = 0$,

$$w^k(x,0) = \boldsymbol{l}^k \cdot \boldsymbol{q}(x,0) = \begin{cases} w_L^k = \boldsymbol{l}^k \cdot \boldsymbol{q}_L & \text{if} \quad x < x_{i+\frac{1}{2}} \\ w_R^k = \boldsymbol{l}^k \cdot \boldsymbol{q}_R & \text{if} \quad x > x_{i+\frac{1}{2}} \end{cases}$$

- In other words, the initial jump $\boldsymbol{q}_R - \boldsymbol{q}_L$ is decomposed in several waves each propagating at the constant speed λ^k and corresponding to the eigenvectors of the Jacobian A:

$$\boldsymbol{q}_R - \boldsymbol{q}_L = \alpha^1 \boldsymbol{r}^1 + \alpha^2 \boldsymbol{r}^2 + \cdots + \alpha^m \boldsymbol{r}^m$$

where $\alpha^k = \boldsymbol{l}^k \cdot (\boldsymbol{q}_R - \boldsymbol{q}_L)$ are the *wave strengths*

The Riemann Problem

- For the linear case, the *exact* solution for each wave at the cell interface is:

$$w^k\left(x_{i+\frac{1}{2}}, t\right) = w^k\left(x_{i+\frac{1}{2}} - \lambda^k t, 0\right) = \begin{cases} w_L^k & \text{if} \quad \lambda^k > 0 \\ w_R^k & \text{if} \quad \lambda^k < 0 \end{cases}$$

- The complete solution is found by adding all wave contributions:

$$\boldsymbol{q}\left(x_{i+\frac{1}{2}}, t\right) = \sum_{k:\lambda_k>0} w_L^k \boldsymbol{r}^k + \sum_{k:\lambda_k<0} w_R^k \boldsymbol{r}^k$$

- and the flux is finally computed as $\tilde{\boldsymbol{F}}_{i+\frac{1}{2}} = A \cdot \boldsymbol{q}\left(x_{i+\frac{1}{2}}, t\right)$

The Riemann Problem

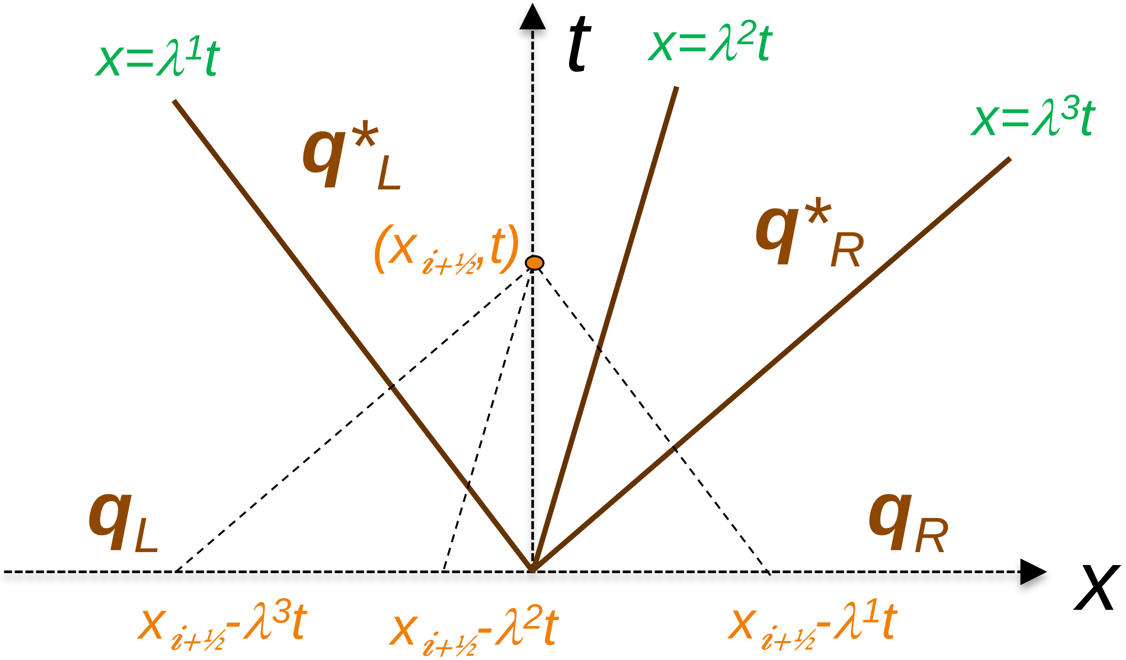

Point (X_0,T) falls to the right of the λ^1 characteristic emanating from the initial jump, but to the left of the other 2, so the solution is:

$$\boldsymbol{q}\left(x_{i+\frac{1}{2}},t\right) = w_R^1\boldsymbol{r}^1 + w_L^2\boldsymbol{r}^2 + w_L^3\boldsymbol{r}^3$$

2d. Basic discretization for hyperbolic PDE: Nonlinear equation

Nonlinear Advection Equation

- We turn our attention to the scalar conservation law

$$\frac{\partial u}{\partial t} + \frac{\partial f(u)}{\partial x} = 0$$

- Where *f(u)* is, in general, a nonlinear function of *u*.

- To gain some insights on the role played by nonlinear effects, we start by considering the inviscid Burger's equation:

$$\frac{\partial u}{\partial t} + \frac{\partial}{\partial x}\left(\frac{u^2}{2}\right) = 0$$

Nonlinear Advection Equation

- We can write Burger's equation also as $$\frac{\partial u}{\partial t} + u\frac{\partial u}{\partial x} = 0$$
- In this form, Burger's equation resembles the linear advection equation, except that the velocity is no longer constant but it is equal to the solution itself.
- The characteristic curve for this equation is

$$\frac{dx}{dt} = u(x,t) \quad \Longrightarrow \quad \frac{du}{dt} = \frac{\partial u}{\partial t} + \frac{\partial u}{\partial x}\frac{dx}{dt} = 0$$

- → u is constant along the curve *dx/dt=u(x,t)* → characteristics are again straight lines: values of *u* associated with some fluid element do not change as that element moves.

Nonlinear Advection Equation

- From $$\frac{\partial u}{\partial t} + u\frac{\partial u}{\partial x} = 0$$

one can predict that, higher values of *u* will propagate faster than lower values: this leads to a wave steepening, since upstream values will advances faster than downstream values.

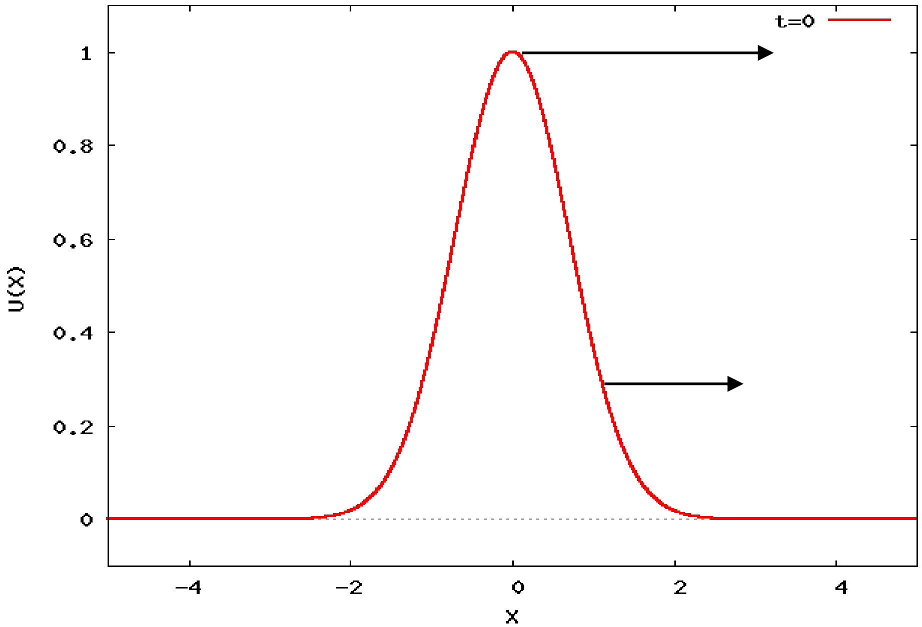

Nonlinear Advection Equation

- Indeed, at t=1 the wave profile will look like:

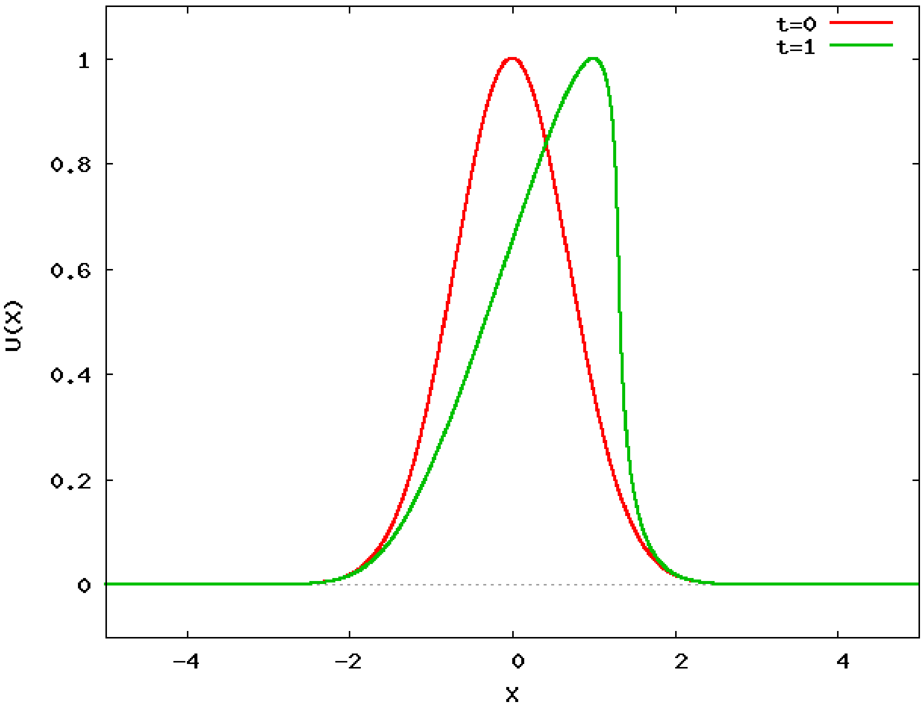

- the wave steepens…

Nonlinear Advection Equation

- If we wait more, we should get something like this:

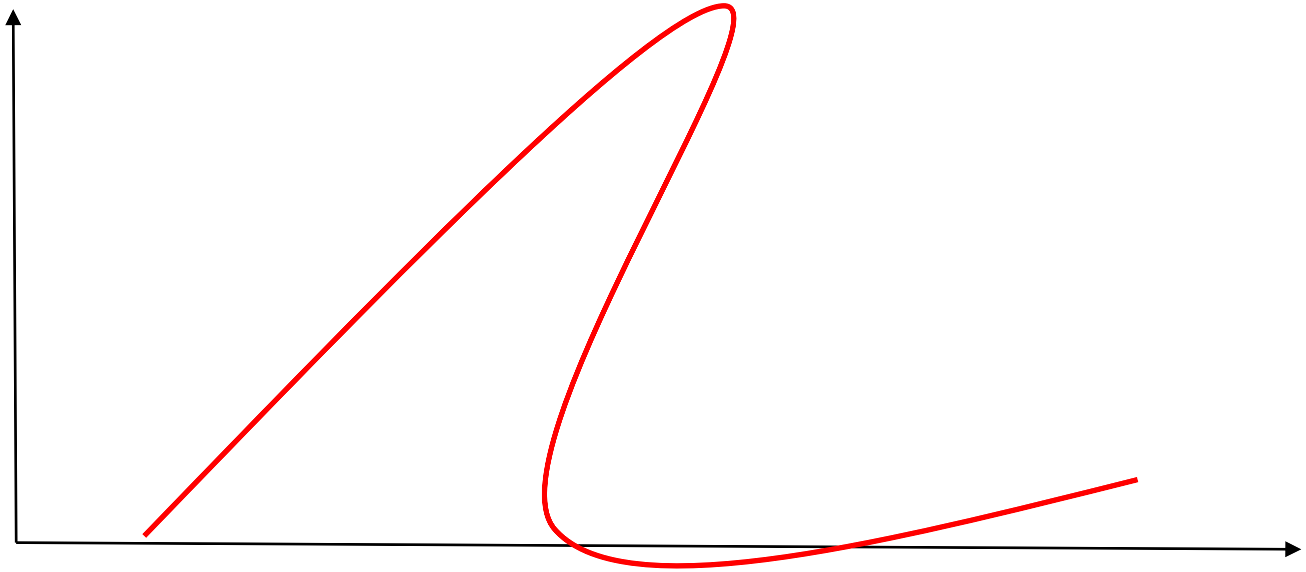

- A multi-value functions ?! → Clearly ***NOT*** physical !

Nonlinear Advection Equation

- The correct physical solution is to place a discontinuity there:

  a *shock wave*.

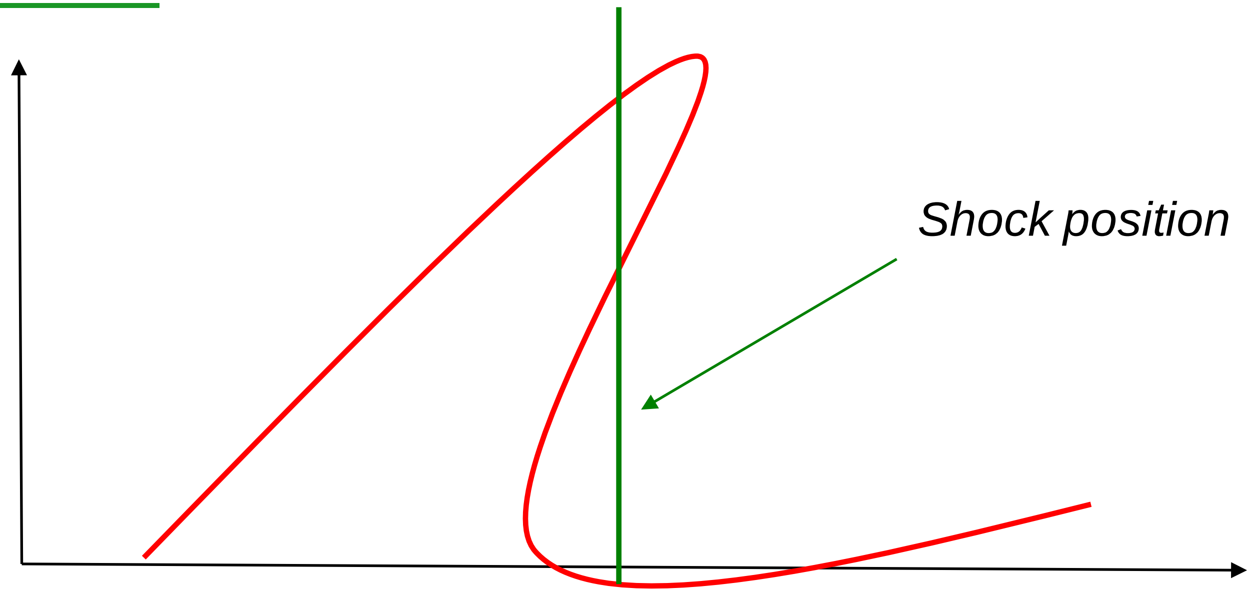

- Since the solution is no longer smooth, the differential form is not valid anymore and we need to consider the *integral form*.

Nonlinear Advection Equation

- This is how the solution should look like:

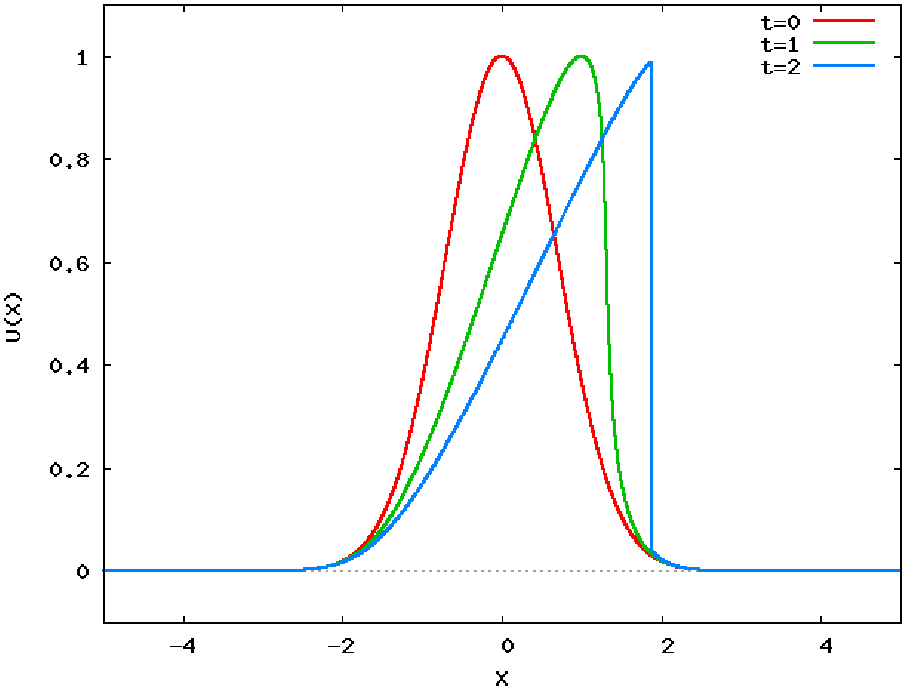

- Such solutions to the PDE are called *weak solutions*.

Nonlinear Advection Equation

- Let's try to understand what happens by looking at the characteristics.
- Consider two states initially separated by a jump at an interface:

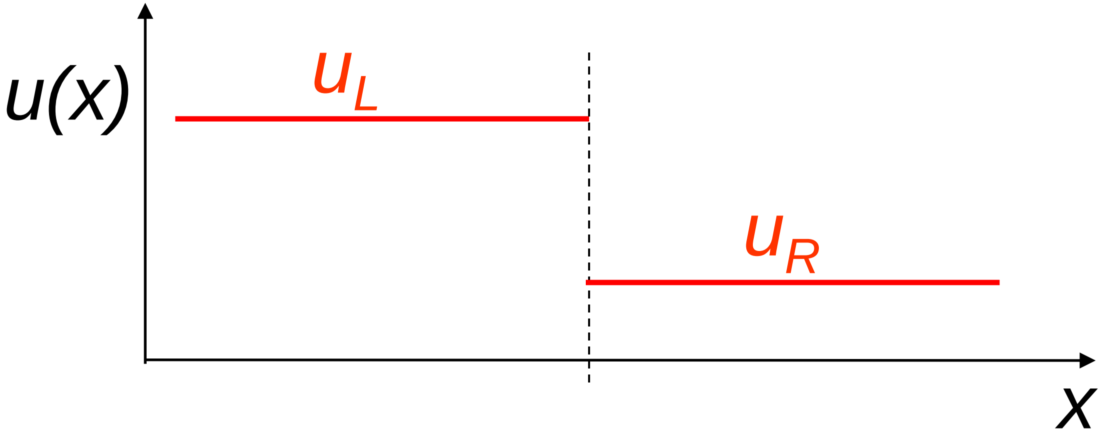

- Here, the characteristic velocities on the left are greater than those on the right.

Nonlinear Advection Equation

- The characteristic will intersect, creating a *shock wave*:

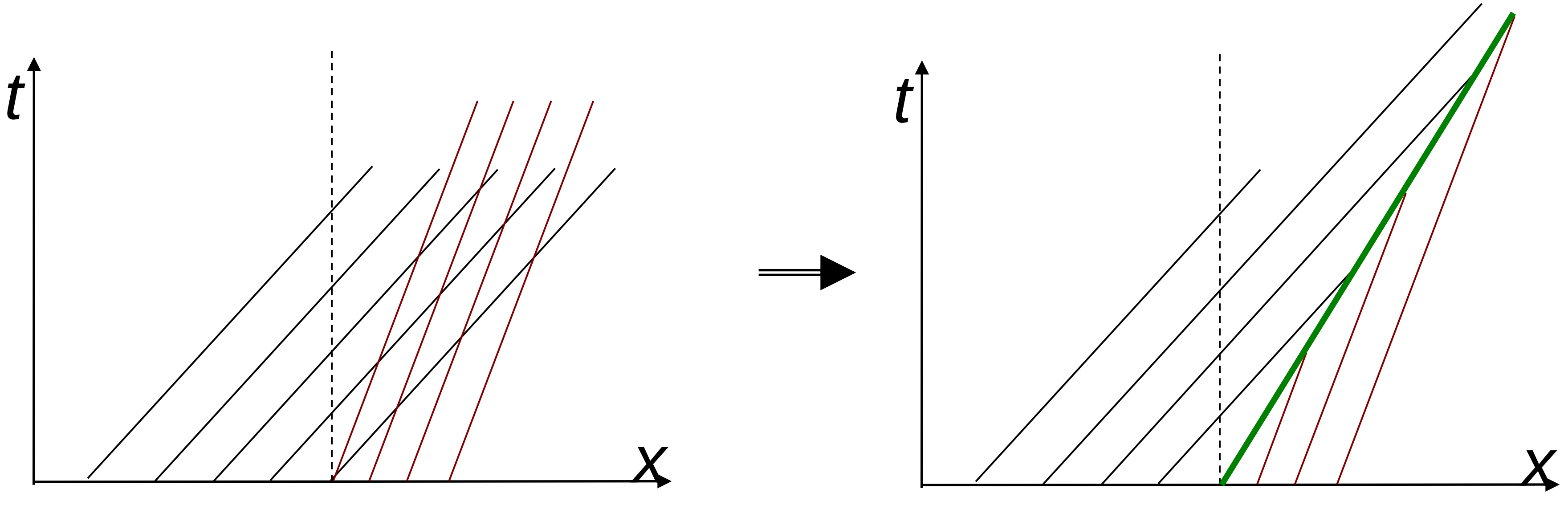

- The shock speed is such that $\lambda(u_L) > S > \lambda(u_R)$. This is called the *entropy condition*.

Nonlinear Advection Equation

- The shock speed S can be found using the Rankine-Hugoniot jump conditions, obtained from the integral form of the equation:

$$f(u_R) - f(u_L) = S(u_R - u_L)$$

- For Burger's equation $f(u) = u^2/2$ so that one finds the shock speed as

$$S = \frac{u_L + u_R}{2}$$

Nonlinear Advection Equation

- Let's consider the opposite situation:

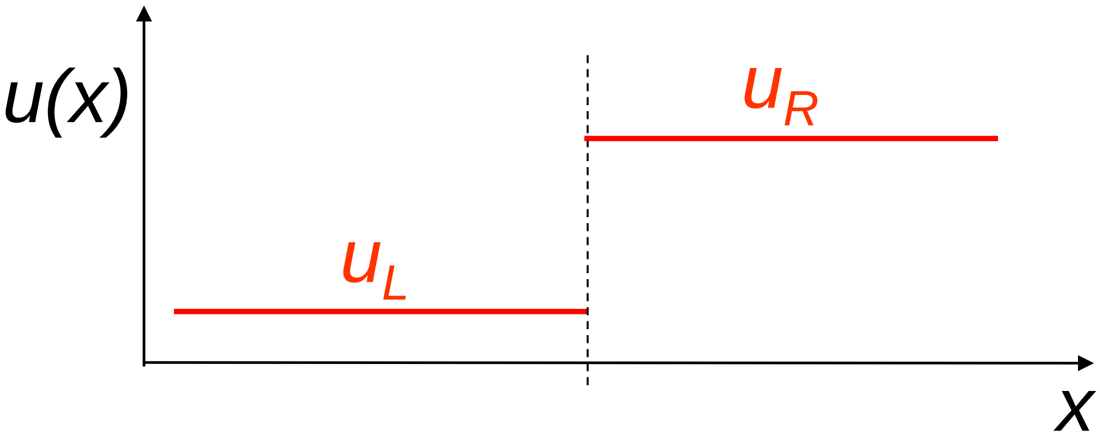

- Here, the characteristic velocities on the left are smaller than those on the right.

Nonlinear Advection Equation

- Now the characteristics will diverge:

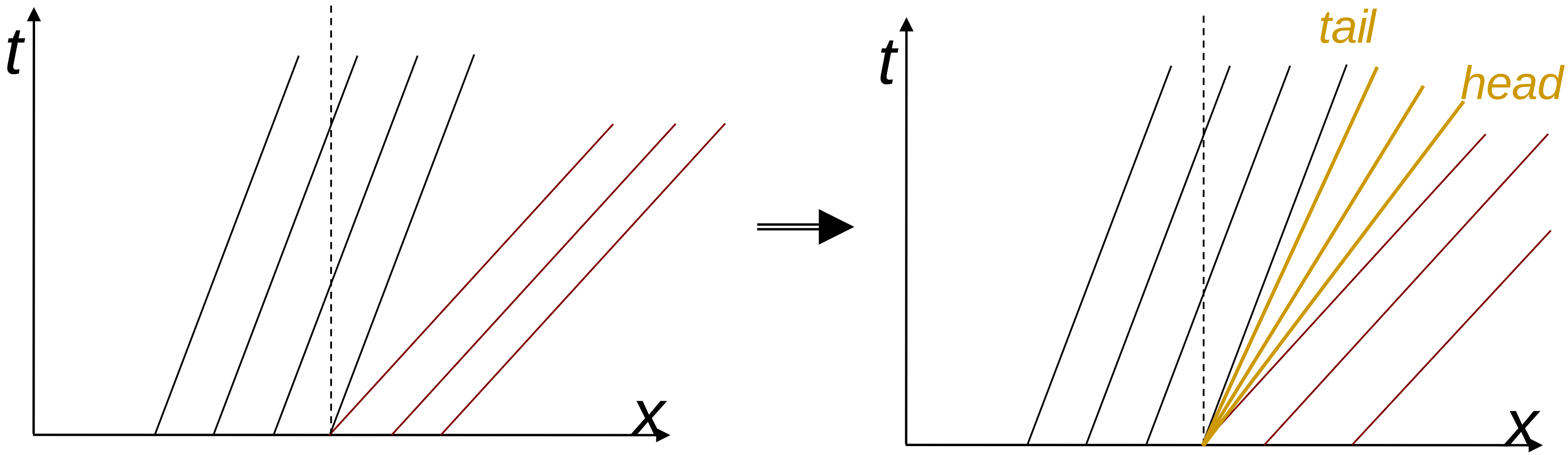

- Putting a shock wave between the two states would be incorrect, since it would violate the entropy condition. Instead, the proper solution is a *rarefaction wave*.

Nonlinear Advection Equation

- A rarefaction wave is a nonlinear wave that smoothly connects the left and the right state. It is an expansion wave.
- The solution between the states can only be self-similar and takes on the range of values between u_L and u_R
- The head of the rarefaction moves at the speed $\lambda(u_R)$, whereas the tail moves at the speed $\lambda(u_L)$.
- The general condition for a rarefaction wave is $\lambda(u_L)<\lambda(u_R)$
- Both rarefactions and shocks are present in the solutions to the Euler equation. Both waves are nonlinear.

Nonlinear Advection Equation

- These results can be used to write the general solution to the Riemann problem for the Burger's equation:
  - If $u_L > u_R$ the solution is a discontinuity (*shock wave)*. In this case

$$u(x,t) = \begin{cases} u_L & \text{if} \quad x - St < 0 \\ u_R & \text{if} \quad x - St > 0 \end{cases}, \qquad S = \frac{u_L + u_R}{2}$$

  - If $u_L < u_R$ the solution is a *rarefaction wave*. In this case

$$u(x,t) = \begin{cases} u_L & \text{if} \quad x/t \le u_L \\ x/t & \text{if} \quad u_L < x/t < u_R \\ u_R & \text{if} \quad x/t > u_R \end{cases}$$

Nonlinear Advection Equation

- Solutions look like

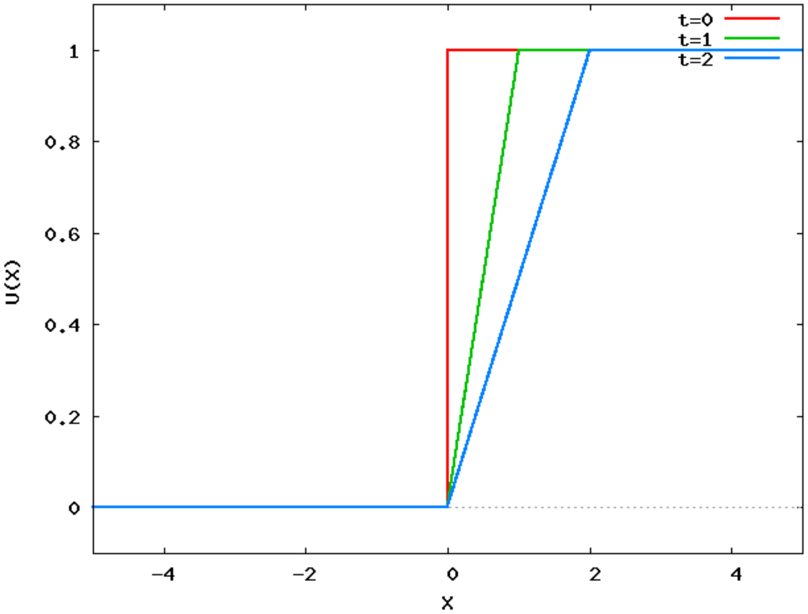

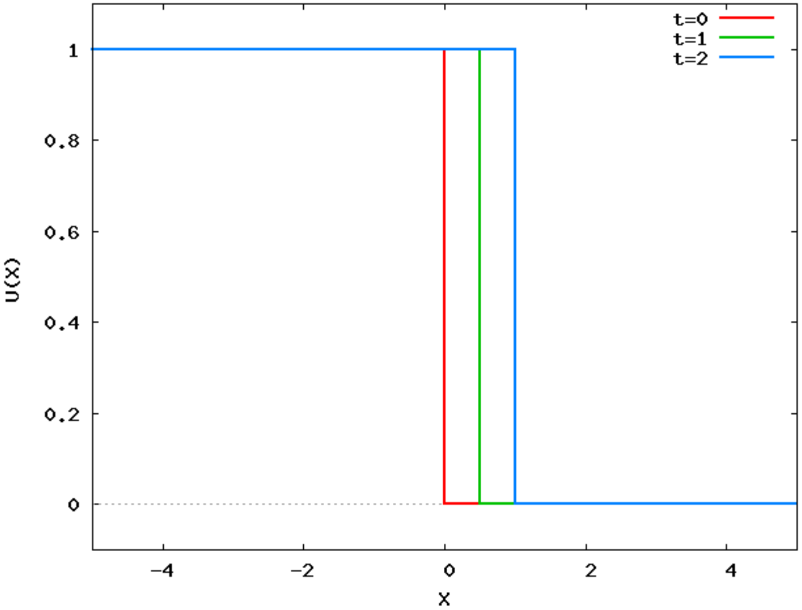

- for a rarefaction and a shock, respectively.

2e. Basic discretization for hyperbolic PDE: Nonlinear Systems

Nonlinear Systems

- Much of what is known about the numerical solution of hyperbolic systems of nonlinear equations comes from the results obtained in the linear case or simple nonlinear scalar equations.

- The key idea is to exploit the conservative form and assume the system can be locally "frozen" at each grid interface.

- However, this still requires the solution of the Riemann problem, which becomes increasingly difficult for complicated set of hyperbolic P.D.E.

Euler Equations

- System of conservation laws describing conservation of mass, momentum and energy:

$$\frac{\partial \rho}{\partial t} + \nabla \cdot (\rho \mathbf{v}) = 0 \qquad \text{(mass)}$$

$$\frac{\partial (\rho \mathbf{v})}{\partial t} + \nabla \cdot [\rho \mathbf{v}\mathbf{v} + \mathbf{I}p] = 0 \qquad \text{(momentum)}$$

$$\frac{\partial E}{\partial t} + \nabla \cdot [(E + p)\, \mathbf{v}] = 0 \qquad \text{(energy)}$$

- Total energy density E is the sum of thermal + Kinetic terms:

$$E = \rho\epsilon + \rho\frac{\mathbf{v}^2}{2}$$

- Closure requires an Equation of State (EoS). For an ideal gas one has

$$\rho\epsilon = \frac{p}{\Gamma - 1}$$

Euler Equations: Characteristic Structure

- The equations of gasdynamics can also be written in "quasi-linear" or primitive form. In 1D:

$$\frac{\partial \mathbf{V}}{\partial t} + A \cdot \frac{\partial \mathbf{V}}{\partial x} = 0\,, \quad A = \left(\begin{array}{ccc} v_x & \rho & 0 \\ 0 & v_x & 1/\rho \\ 0 & \rho c_s^2 & v_x \end{array}\right)$$

where $V = [\rho, v_x, p]$ is a vector of primitive variable, $c_s = (\gamma p/\rho)^{1/2}$ is the adiabatic speed of sound.

- It is called "quasi-linear" since, differently from the linear case where we had $A=const$, here $A = A(V)$.

Euler Equations: Characteristic Structure

- The quasi-linear form can be used to find the eigenvector decomposition of the matrix *A*:

$$\mathbf{r}^1 = \begin{pmatrix} 1 \\ -c_s/\rho \\ c_s^2 \end{pmatrix}, \quad \mathbf{r}^2 = \begin{pmatrix} 1 \\ 0 \\ 0 \end{pmatrix}, \quad \mathbf{r}^3 = \begin{pmatrix} 1 \\ c_s/\rho \\ c_s^2 \end{pmatrix}$$

- Associated with the eigenvalues:

$$\lambda^1 = v_x - c_s\,, \quad \lambda^2 = v_x\,, \quad \lambda^3 = v_x + c_s$$

- These are the characteristic speeds of the system, i.e., the speeds at which information propagates. They tell us a lot about the structure of the solution.

Euler Equations: Riemann Problem

- By looking at the expressions for the right eigenvectors,

$$\mathbf{r}^1 = \begin{pmatrix} 1 \\ -c_s/\rho \\ c_s^2 \end{pmatrix}, \quad \mathbf{r}^2 = \begin{pmatrix} 1 \\ 0 \\ 0 \end{pmatrix}, \quad \mathbf{r}^3 = \begin{pmatrix} 1 \\ c_s/\rho \\ c_s^2 \end{pmatrix}$$

- we see that across waves 1 and 3, all variables jump. These are nonlinear waves, either *shocks* or *rarefactions waves*.

- Across wave 2, only the density jumps. Velocity and pressure are constant. This defines the contact discontinuity.

- The characteristic curve associated with this linear wave is $dx/dt = u$, and it is a straight line. Since v_x is constant across this wave, the flow is neither converging or diverging.

Euler Equations: Riemann Problem

- The solution to the Riemann problem looks like

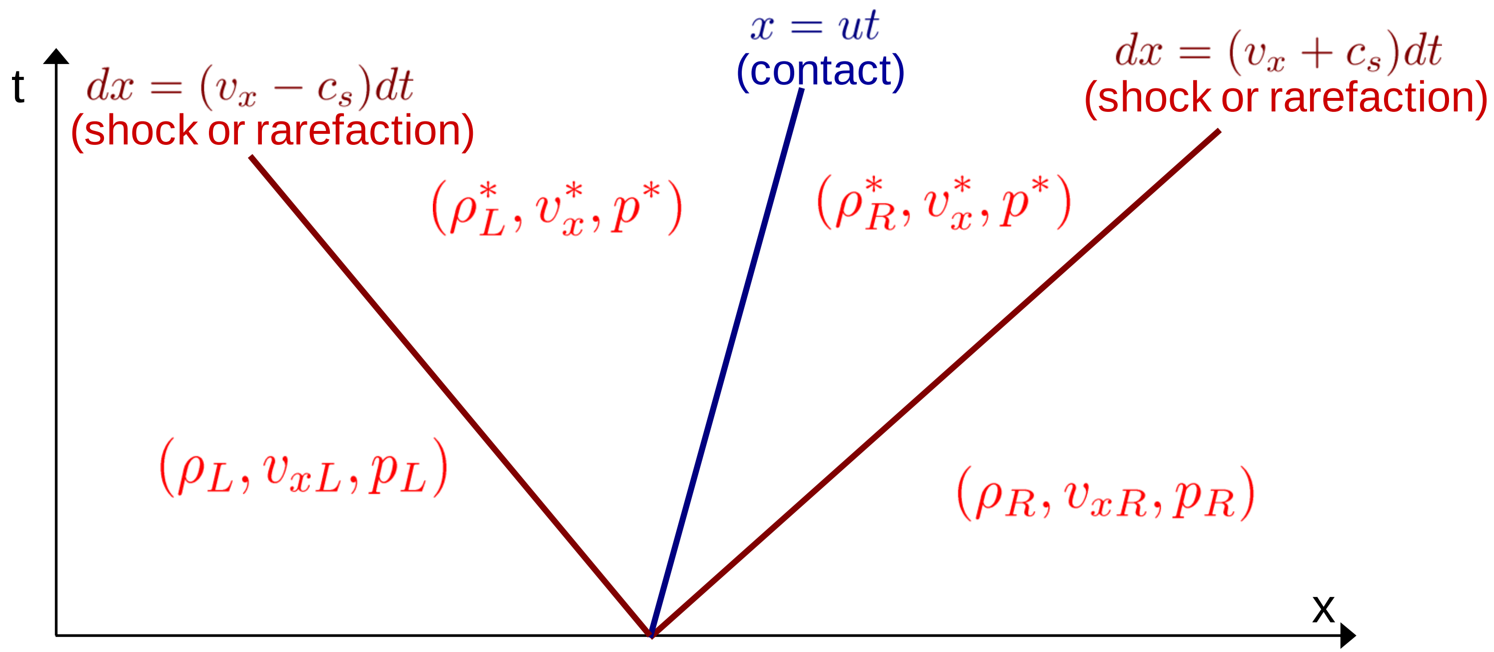

- The outer waves can be either shocks or rarefactions.
- The middle wave is always a contact discontinuity.
- In total one has 4 unknowns: $\rho_L^*, \rho_R^*, v_x^*, p^*$ since only density jumps across the contact discontinuity.

Euler Equations: Riemann Problem

- Depending on the initial discontinuity, a total of 4 patterns can emerge from the solution:

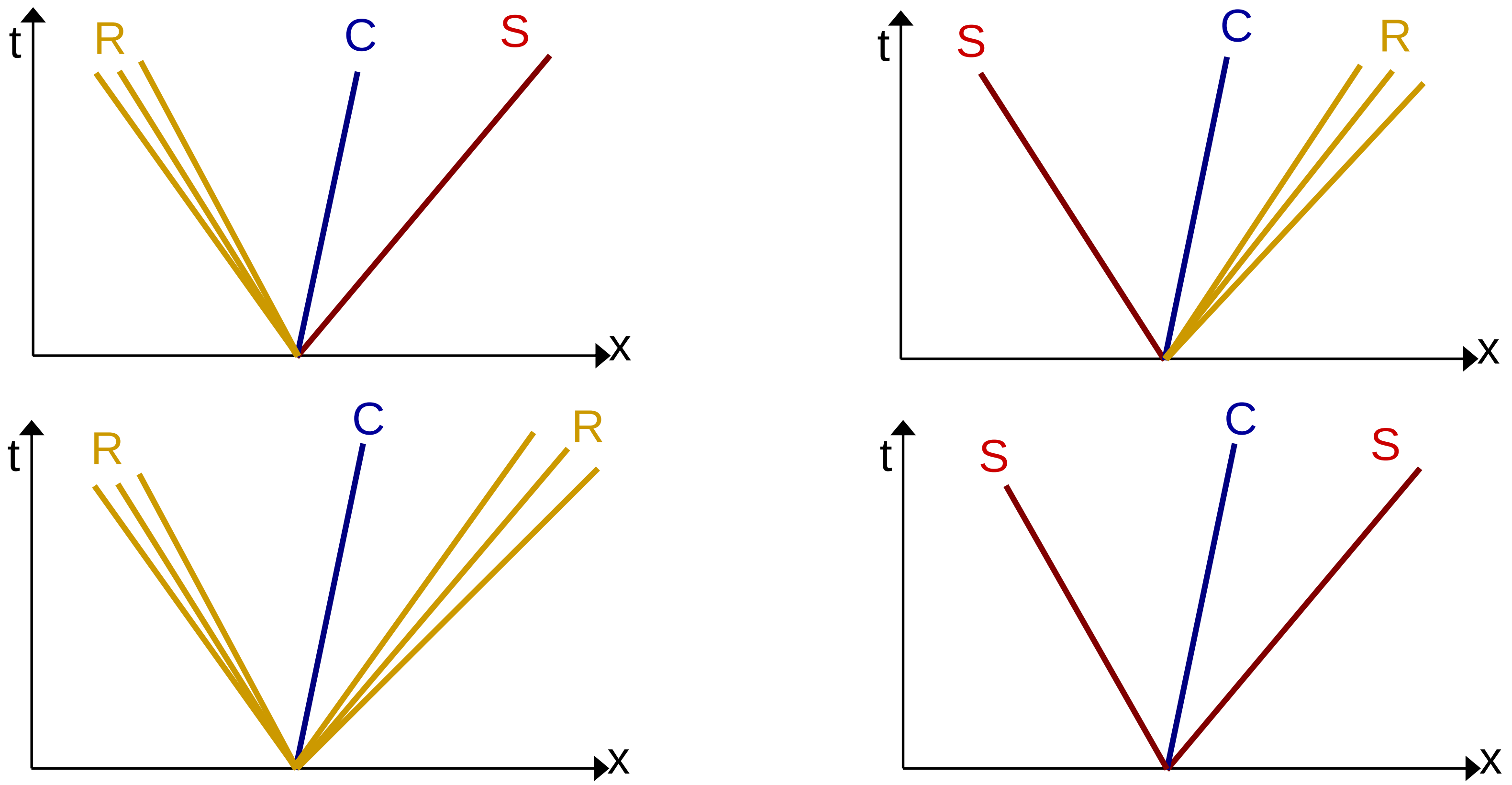

Euler Equations: Shock Tube Problem

- The decay of the discontinuity defines what is usually called the “shock tube problem”,

- Left Values:

$$(\rho_L, v_{xL}, p_L) = (1, 0, 1)$$

- Right Values:

$$(\rho_R, v_{xR}, p_R) = \left(\frac{1}{8}, 0, \frac{1}{10}\right)$$

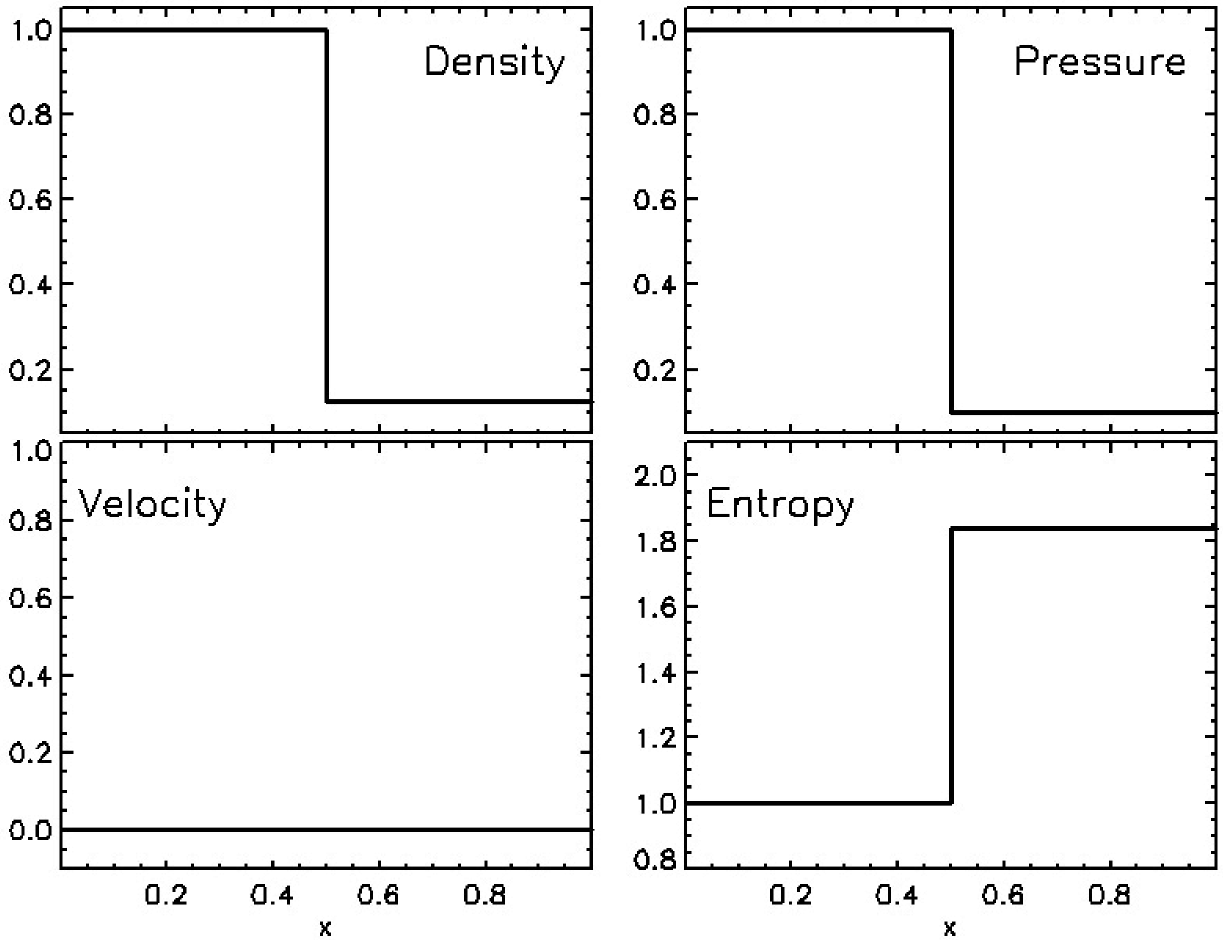

Euler Equations: Shock Tube Problem

- The one dimensional jet problem reduces to a shock-tube with a S-C-S structure:

- Left Values:

$$(\rho_L, v_{xL}, p_L) = (0.1, 10, 1)$$

- Right Values:

$$(\rho_R, v_{xR}, p_R) = (1, 0, 1)$$

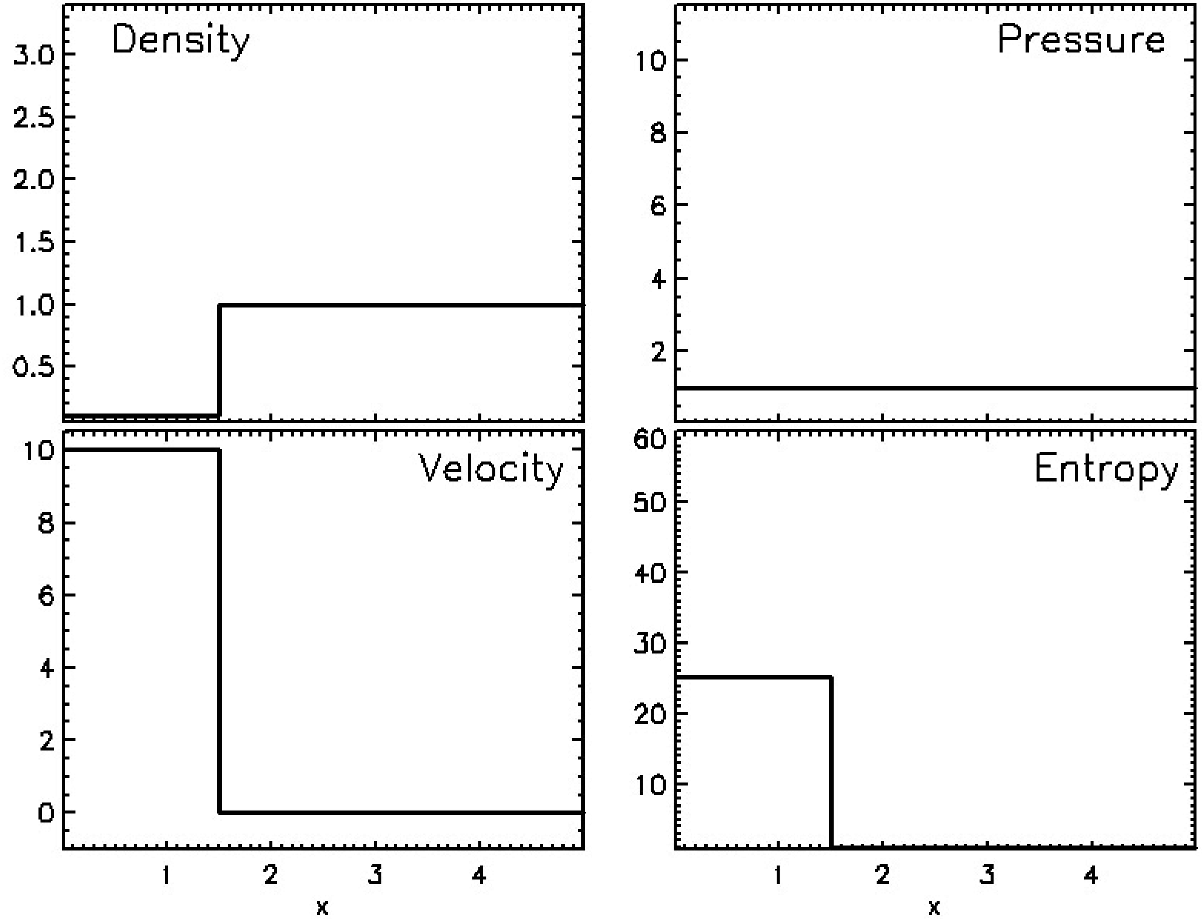

Riemann Problem in MHD

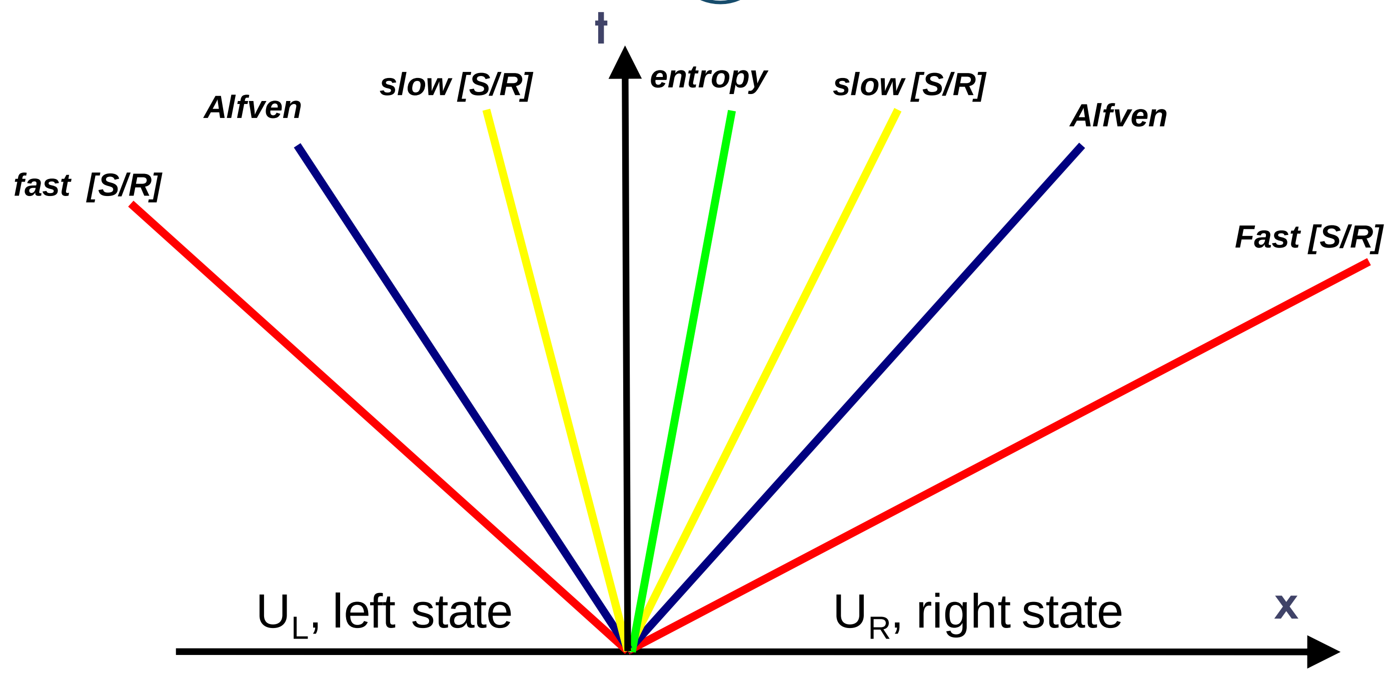

- 7 wave pattern, $\lambda^{(\kappa)}\left(\boldsymbol{U}_L^{(\kappa)} - \boldsymbol{U}_R^{(\kappa)}\right) = \boldsymbol{F}\left(\boldsymbol{U}_L^{(\kappa)}\right) - \boldsymbol{F}\left(\boldsymbol{U}_R^{(\kappa)}\right)$
- across the contact wave, for $B_n \neq 0$, only density has a jump;
- across Alfven waves, $[\rho]=[p_{gas}]=[v_x]=0$

An example

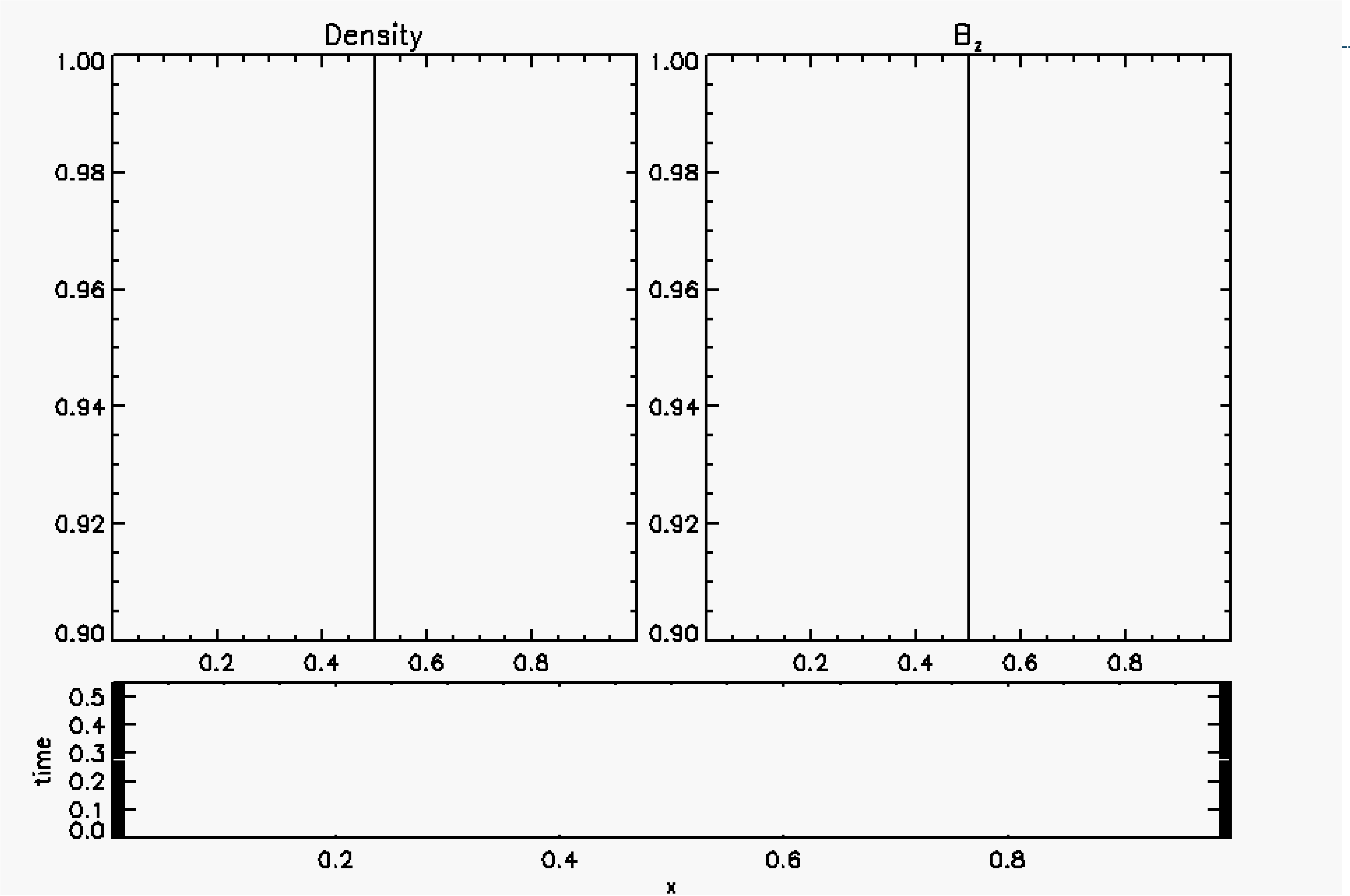

Density
B_z
1.00
0.98
0.96
0.94
0.92
0.90
0.2
0.4
0.6
0.8
time
0.5
0.4
0.3
0.2
0.1
0.0
x

Solving the Riemann Problem

- The full analytical solution to the Riemann problem for the Euler equation can be found, but this is a rather complicated task (see the book by Toro).

- In general, approximate methods of solution are preferred.

- The advantage of using approximate solvers is the reduced computational costs and the ease of implementation.

- The degree of approximation reflects on the ability to "capture" and spread discontinuities over few or more computational zones.

Solving the Riemann Problem

- ***Exact** Riemann solvers* (nonlinear)
  - Full nonlinear solution:
  - Expensive / impracticable for heavily usage in upwind codes;

- ***Linearized** Riemann solvers* (Roe type)
  - require characteristic decomposition in eigenvectors
  - may be prone to numerical pathologies

- ***HLL-type** Riemann solvers* (guess-based)
  - based on guess to the signal speeds and on the integral average of the solution over the Riemann Fan;
  - fewer waves are considered in the solution;
  - preserve positivity;

Resolution of Contact Discontinuity

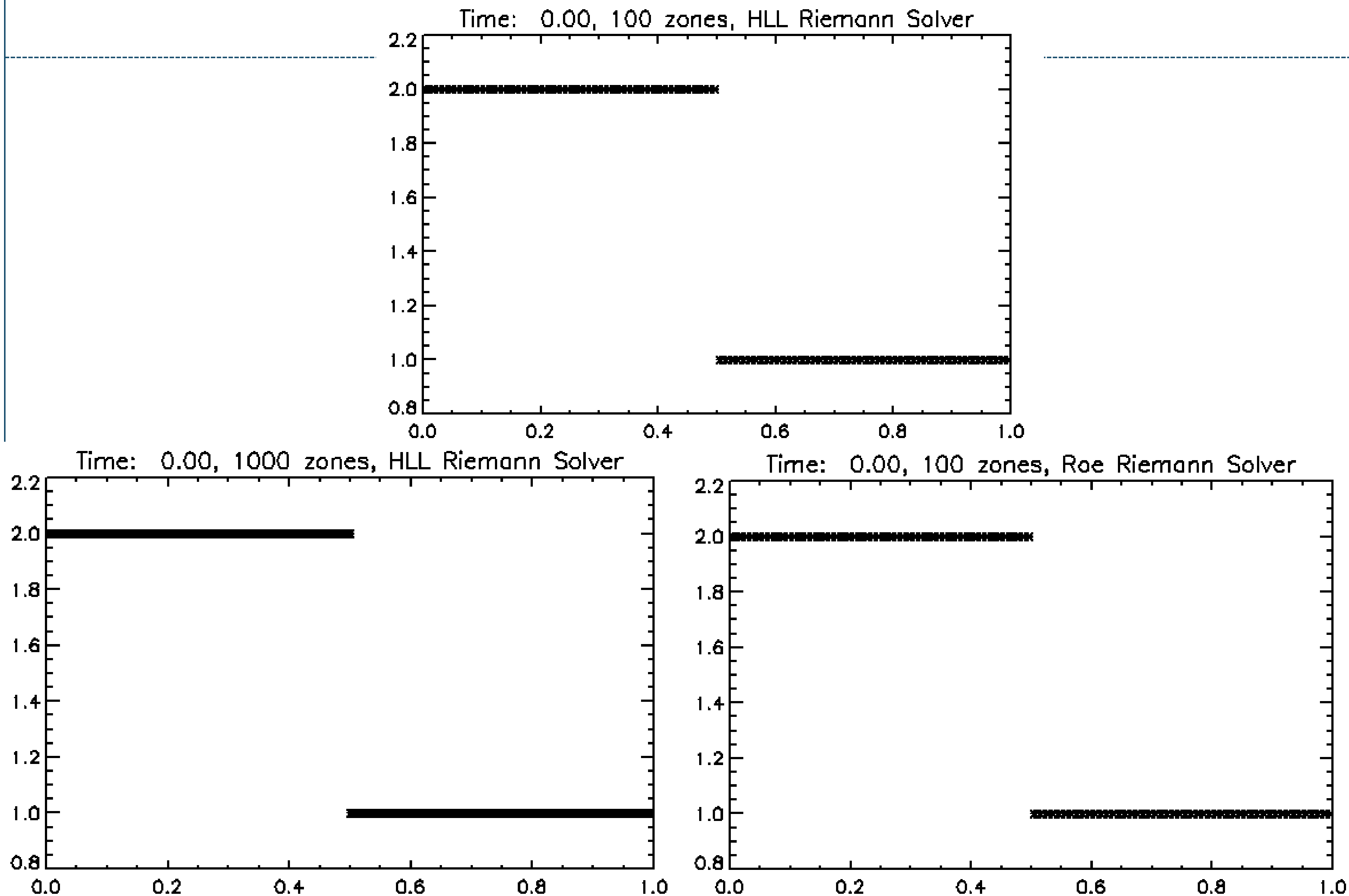

Example: Kelvin-Helmholtz Instability

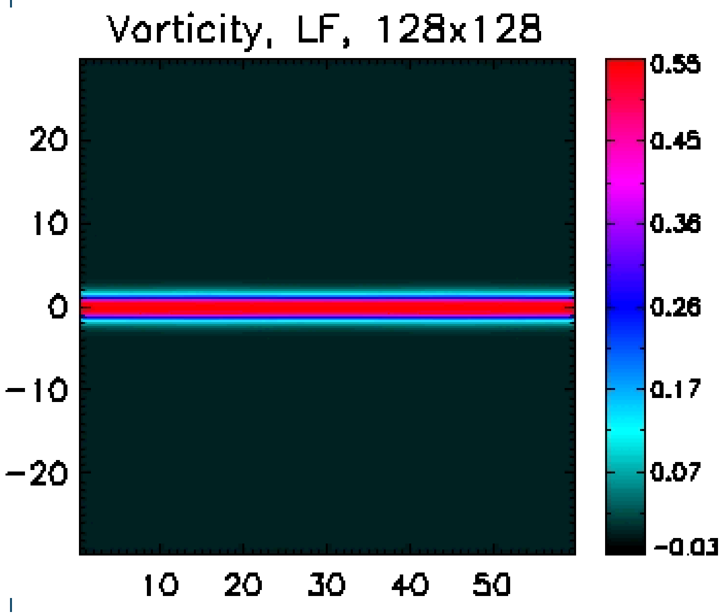

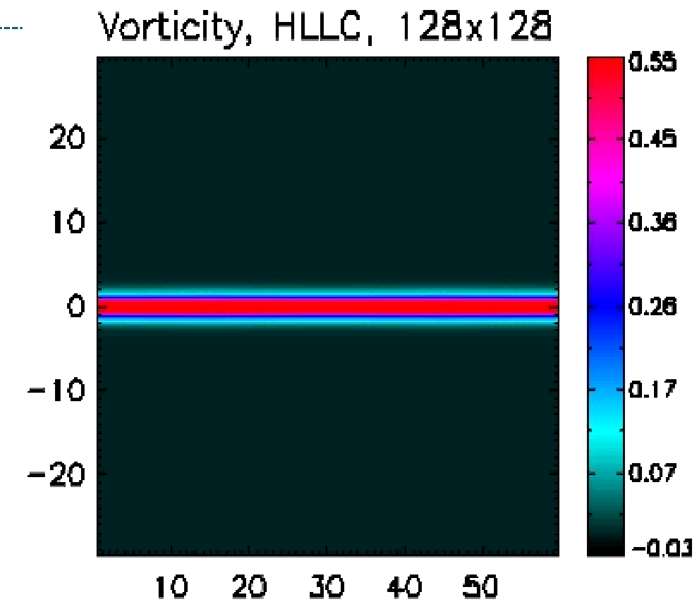

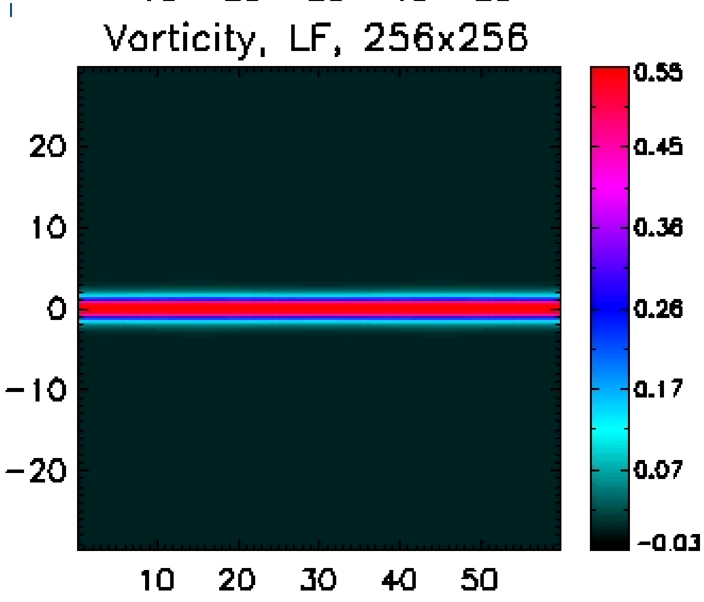

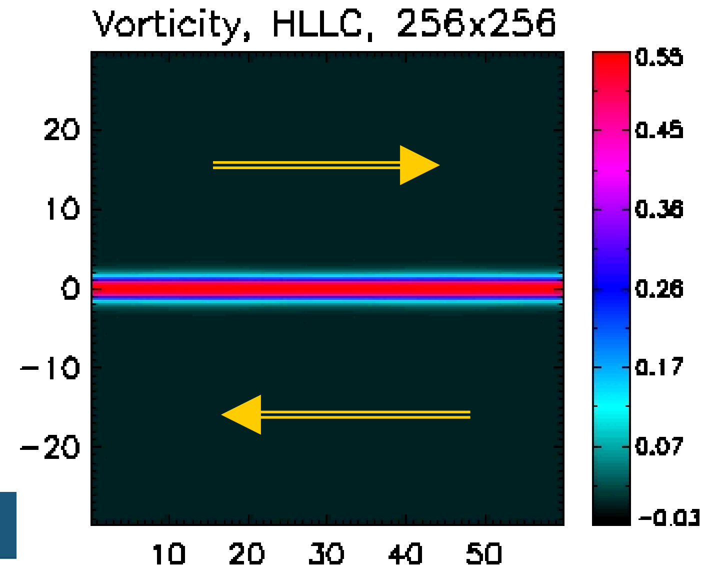

2f. Basic discretization for hyperbolic PDE: High-order Schemes

High order Integration in time

- A simple and effective way to achieve 2nd or 3rd order accuracy in time is to treat the PDE in semi-discrete form:

$$\int \left(\frac{\partial \boldsymbol{q}}{\partial t} + \nabla \cdot \boldsymbol{F} \right) dV = 0 \quad \Longrightarrow \quad \frac{d\bar{\boldsymbol{q}}}{dt} = -\oint \tilde{\boldsymbol{F}} \cdot d\boldsymbol{S}$$

- In such a way the PDE becomes a regular ordinary differential equation (ODE) in time;

$$\frac{d\bar{\boldsymbol{q}}}{dt} = \boldsymbol{R}(\boldsymbol{q}, t) = \boldsymbol{R} \quad \Longrightarrow \quad \bar{\boldsymbol{q}}^{n+1} - \bar{\boldsymbol{q}}^{n} = \int_{n}^{n+1} \boldsymbol{R}\, dt$$

- Standard integration based on predictor/corrector schemes can then be used to solve ODEs.

Second-order Runge-Kutta

- Using the trapezoidal method, the solution of our ODE writes:

$$\bar{\boldsymbol{q}}^{n+1} = \bar{\boldsymbol{q}}^{n} + \frac{\Delta t}{2}\left(\boldsymbol{R}^{n} + \boldsymbol{R}^{n+1}\right) + O(\Delta t^3)$$

- Problem: the unknown $\bar{\boldsymbol{q}}^{n+1}$ppears on both side of the equation!!!
- Solution: use an estimate (predictor) for $\boldsymbol{R}^{n+1}$vith Euler method:

$$\begin{aligned} \bar{\boldsymbol{q}}^{*} &= \bar{\boldsymbol{q}}^{n} + \Delta t \boldsymbol{R}^{n} + O(\Delta t^2) \\ \bar{\boldsymbol{q}}^{n+1} &= \bar{\boldsymbol{q}}^{n} + \frac{\Delta t}{2}\left(\boldsymbol{R}^{n} + \boldsymbol{R}^{*}\right) + O(\Delta t^3) \end{aligned}$$

- This is the second-order explicit Runge-Kutta method (or Heun’s method) It is 2nd order accurate.

Improving spatial accuracy

- High order reconstruction can be carried inside each cell by suitable oscillation-free polynomial interpolation:

Piecewise constant

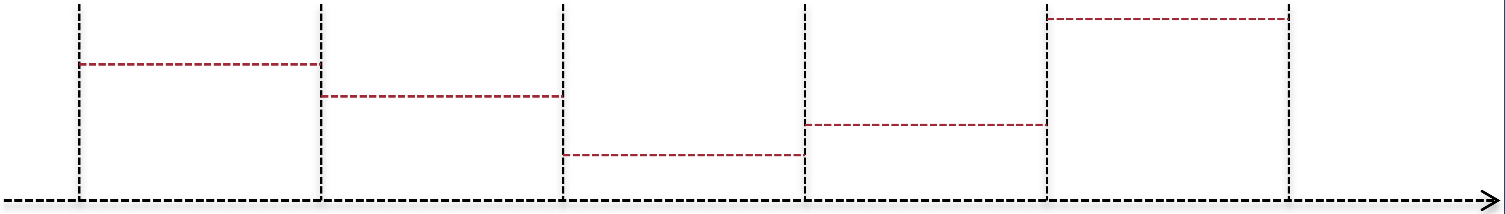

Piecewise Linear

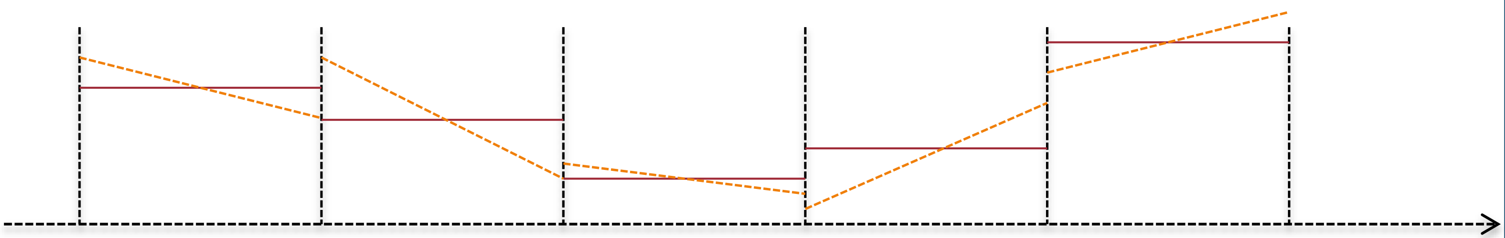

Piecewise parabolic

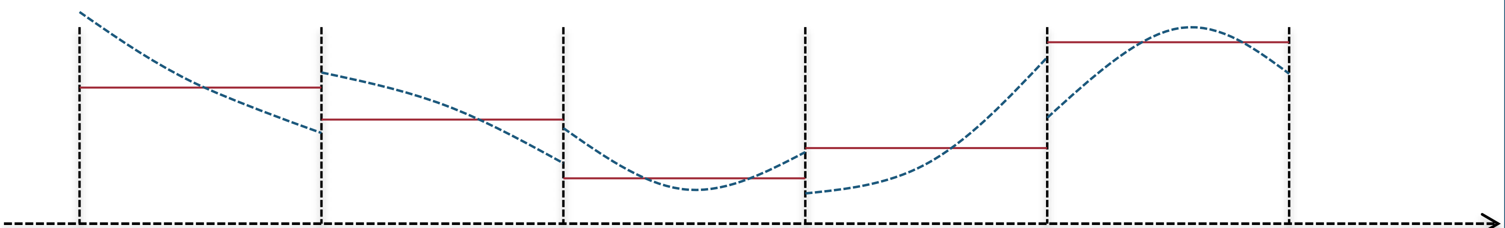

Reconstruction Constraints

- Must be consistent with data representation

$$\frac{1}{\Delta x_i}\int_{x_{i-\frac{1}{2}}}^{x_{i+\frac{1}{2}}} P_i(x)dx = \bar{u}_i$$

- Satisfy monotonicity constraints:

$$\min(P_i(x)) \geq \min\left(\bar{u}_{i-1}, \bar{u}_i, \bar{u}_{i+1}\right)$$
$$\max(P_i(x)) \leq \max\left(\bar{u}_{i-1}, \bar{u}_i, \bar{u}_{i+1}\right)$$

- no new extrema allowed (Total Variation Diminishing (TVD) schemes)
- Oscillation free solution

Example: 2nd order linear reconstruction

- For 2nd-order interpolant, we use

$$V(x) = V_i + \frac{\delta V}{\Delta x}(x - x_i)$$

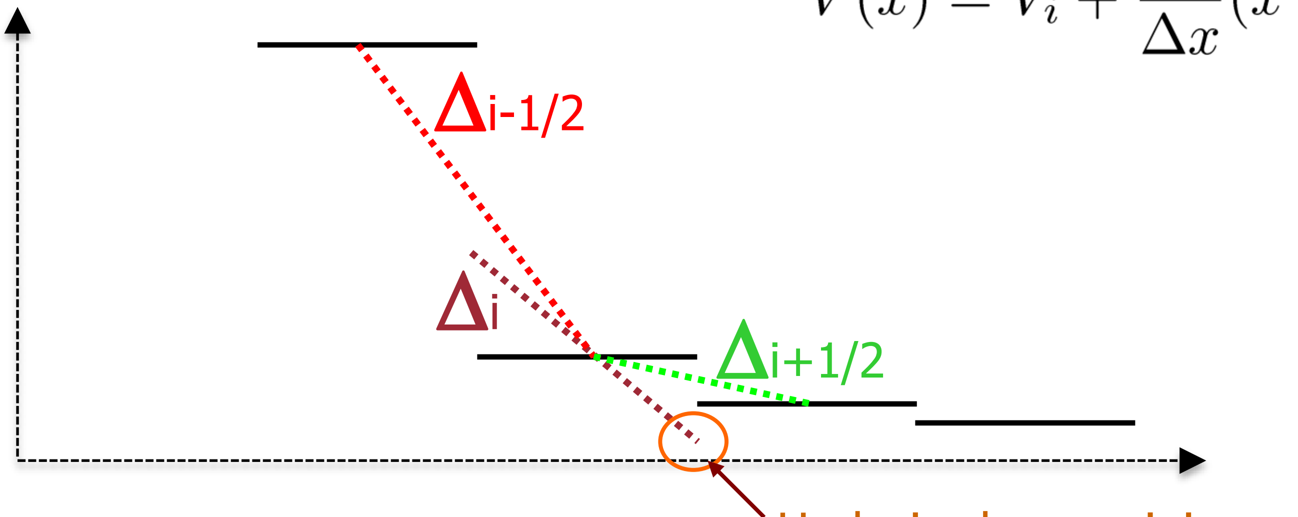

- Use slope limiters to avoid introducing new extrema:

$$\delta V_i = \lim\left(\Delta_{\mathrm{i}-1/2}, \Delta_{\mathrm{i}+1/2}\right)$$

- Example

$$\mathrm{minmod}(x,y) = \begin{cases} x & \text{if} \quad |x| < |y|, xy > 0 \\ y & \text{if} \quad |y| < |x|, xy > 0 \\ 0 & \text{if} \quad xy < 0 \end{cases}$$

Comparison

- Improving reconstruction decreases the amount of numerical dissipation:

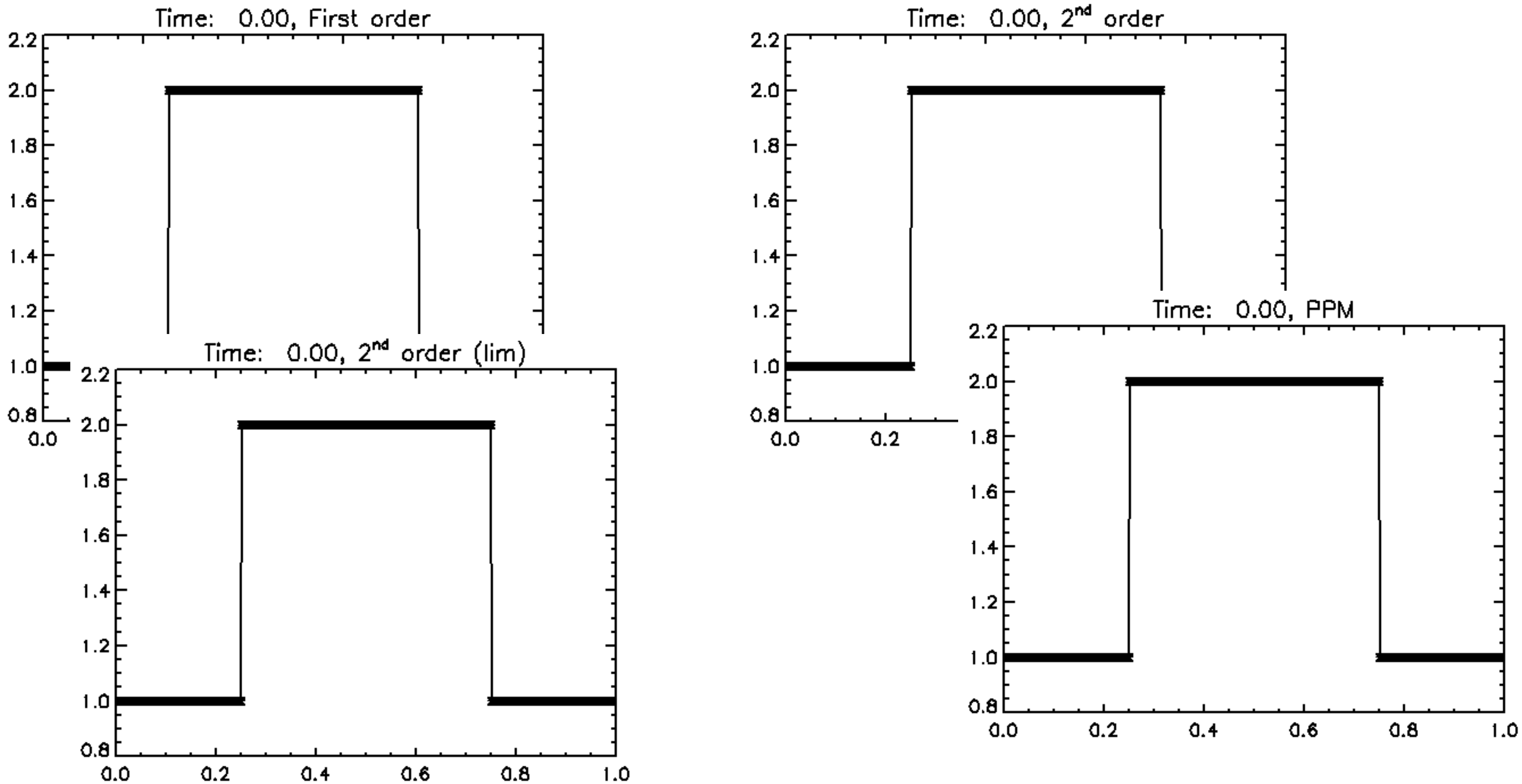

Equivalent advection/diffusion equation

- A discretized PDE gives the exact solution to an equivalent equation with a diffusion term;

- Consider $$\frac{\partial q}{\partial t} + a\frac{\partial q}{\partial x} = 0\,, \qquad a > 0$$
  - Use upwind discretization: $$\frac{q_i^{n+1} - q_i^n}{\Delta t} + a\frac{q_i^n - q_{i-1}^n}{\Delta x} = 0$$
  - Do Taylor expansion on q_i^{n+1} and q_{i-1}^n
  - The solution to the discretized equation satisfies *exactly*

$$\frac{\partial q}{\partial t} + a\frac{\partial q}{\partial x} = \frac{a\Delta x}{2}\left(1 - a\frac{\Delta t}{\Delta x}\right)\frac{\partial^2 q}{\partial x^2} + H.O.T.$$

Reconstruct-Solve-Average

- Start from zone averages, break the problem into 3 pieces:

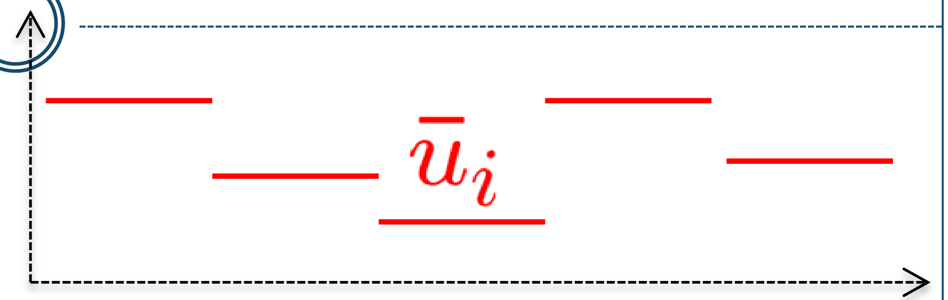

1. Piecewise polynomial reconstruction

$$u_i(x) = P_i(x)\,, \text{ for } x_{i-\frac{1}{2}} < x < x_{i+\frac{1}{2}}$$

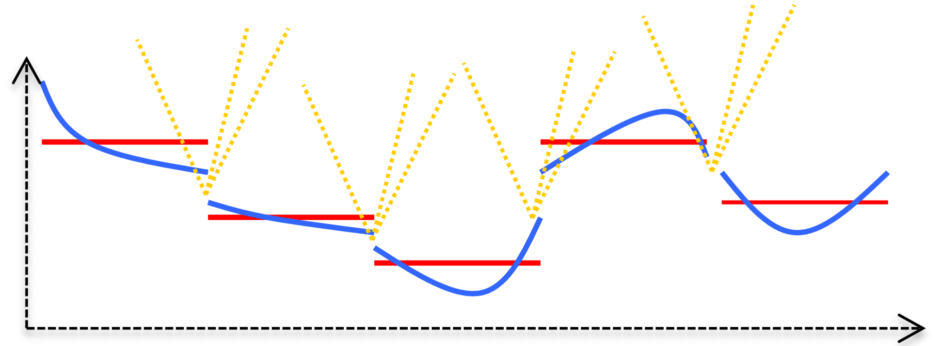

2. Solve Riemann problem between left and right states

$$\begin{cases} u_L = P_i\left(x_{i+\frac{1}{2}}\right) \\ u_R = P_{i+1}\left(x_{i+\frac{1}{2}}\right) \end{cases} \longrightarrow f_{i+\frac{1}{2}}$$

3. Form new averages (evolve)

$$\bar{u}_i^{n+1} = \bar{u}_i^n - \frac{\Delta t}{\Delta x}\left[f_{i+\frac{1}{2}} - f_{i-\frac{1}{2}}\right]$$

Multi Dimensional Integration

- Integration in more than one dimensions can be achieved using two distinct approaches:

  - Dimensionally Split schemes: solve the PDE as a sequence of 1-D sub-problems.

$$\mathbf{q}^* = \mathbf{q}^n - \Delta t \mathcal{L}_x(\mathbf{q}^n) \qquad \mathbf{q}^{n+1} = \mathbf{q}^* - \Delta t \mathcal{L}_y(\mathbf{q}^*)$$

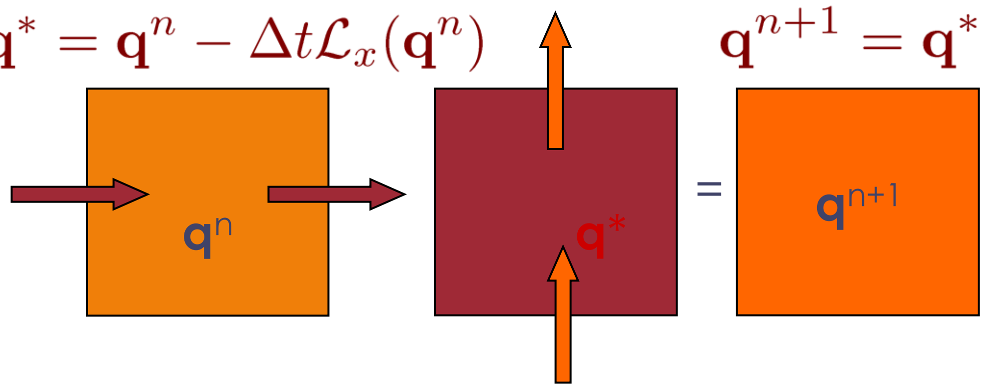

  - Dimensionally Unsplit schemes: solve the full problem:

$$\mathbf{q}^{n+1} = \mathbf{q}^n - \Delta t \mathcal{L}_x(\mathbf{q}^n) - \Delta t \mathcal{L}_y(\mathbf{q}^n)$$

3a. Astrophysical Applications: Accretion Disks

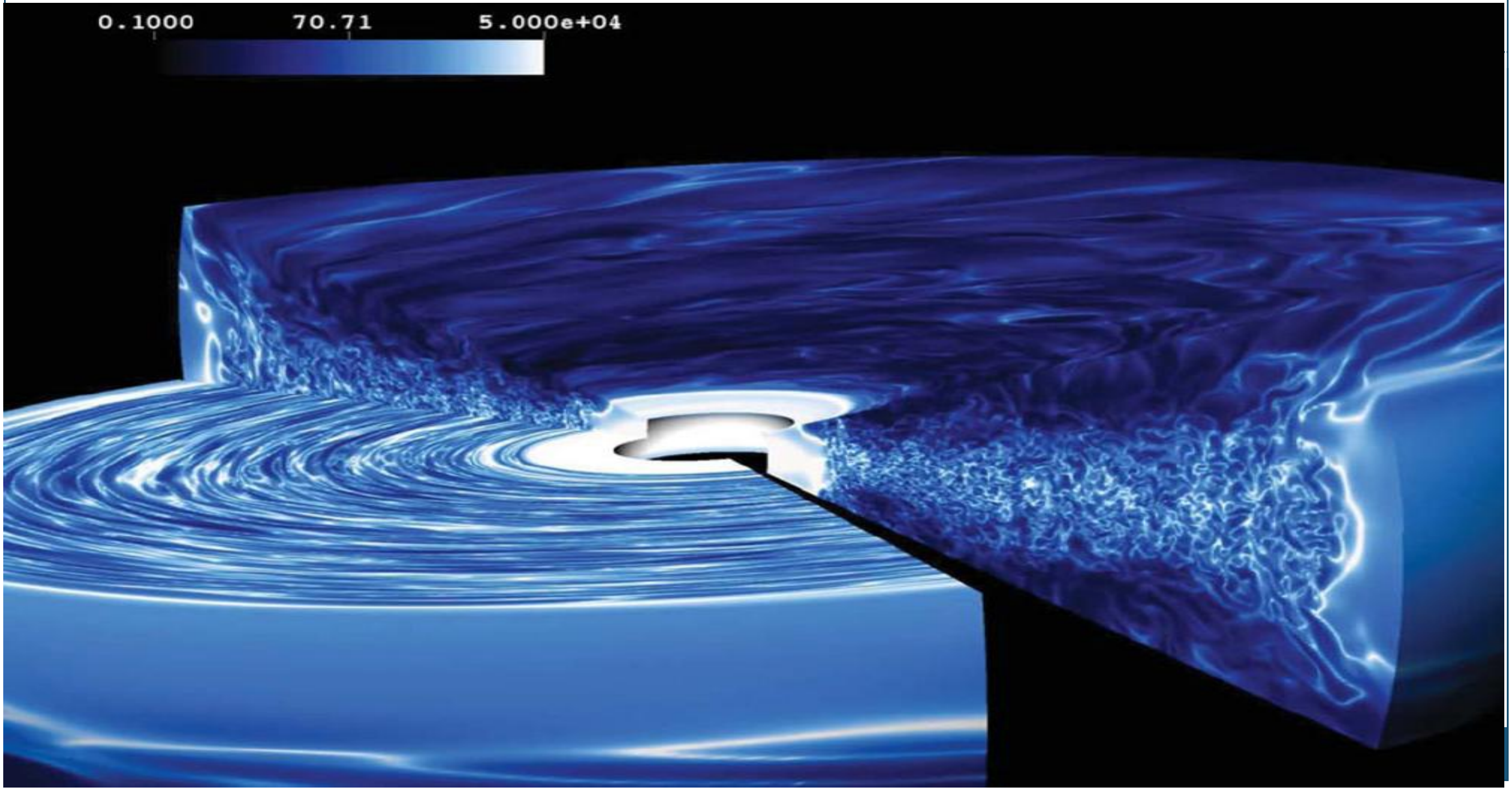

Accretion Disks: open problems

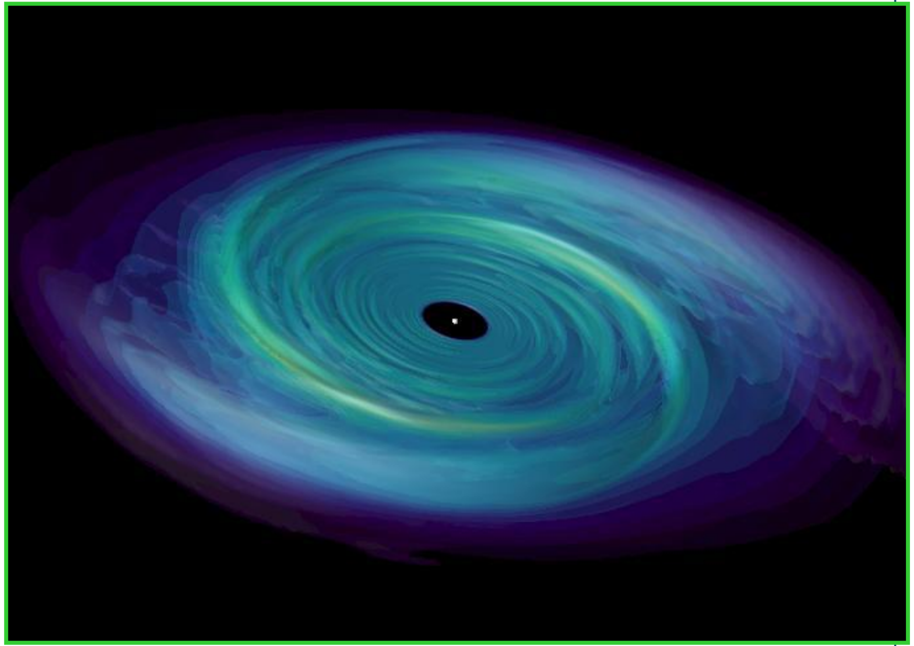

- Accretion disks form because gas falling onto a gravitating object inevitably has some angular momentum (*a.m.*) that forces it to orbit around the object;

- Gravity causes material to spiral inward towards the central body only if *a.m.* is transported outwards;

- Infalling matter must loose gravitational energy and momentum: *Angular momentum extraction at the origin of the jet paradigm*.

[1]Shakura & Sunyaev, 1973; [2]Velikhov 1959; [3]Chandrasekhar 1960; [4]Balbus & Hawley (1990)

Accretion Disks: open problems

- Turbulence possible source of angular momentum transport in accretion disks[1];

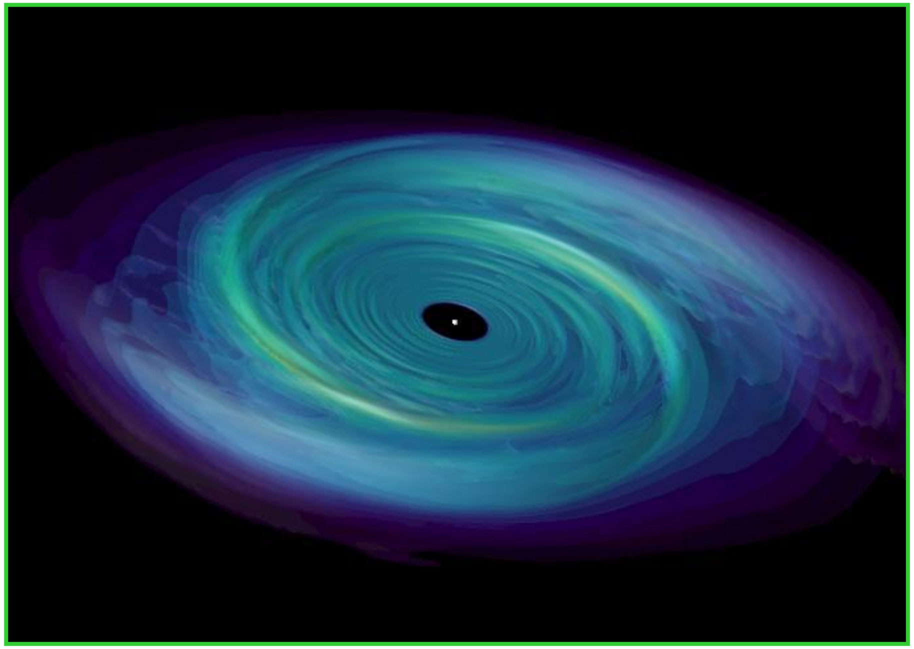

- Problem: microscopic viscosity not sufficient
  → turbulent enhanced viscosity
  → what is its origin ?

- Magnetorotational instability (MRI[2,3]) re-discovered by Balbus & Hawley (1991) proposed as the main process at the base of angular momentum transport in accretion disks.

[1]Shakura & Sunyaev, 1973; [2]Velikhov 1959; [3]Chandrasekhar 1960; [4]Balbus & Hawley (1990)

Accretion Disks: axisymmetric models

- To reduce computational cost, previous models adopted considerable simplifications, e.g., axisymmetry:

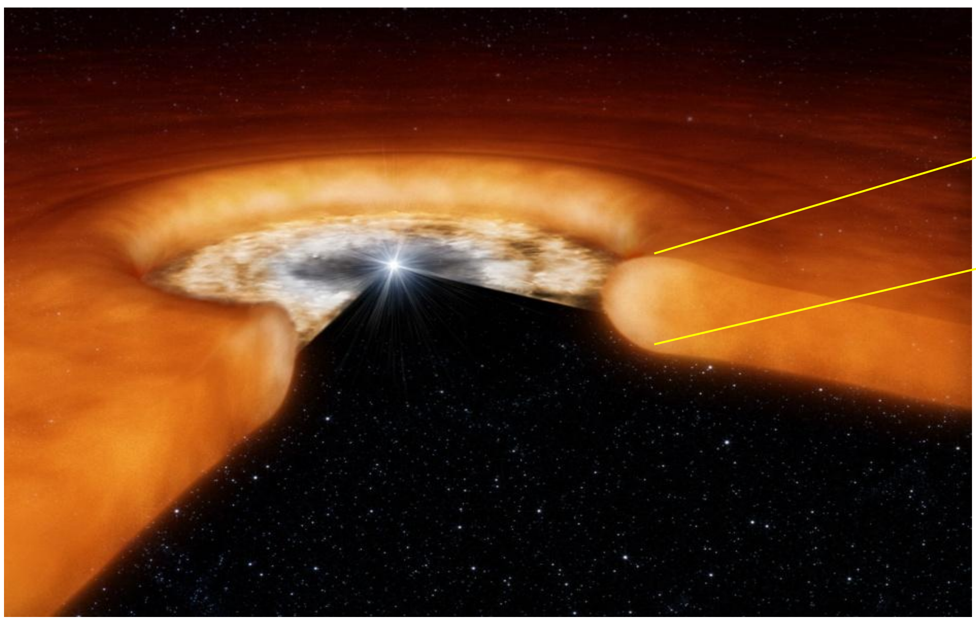

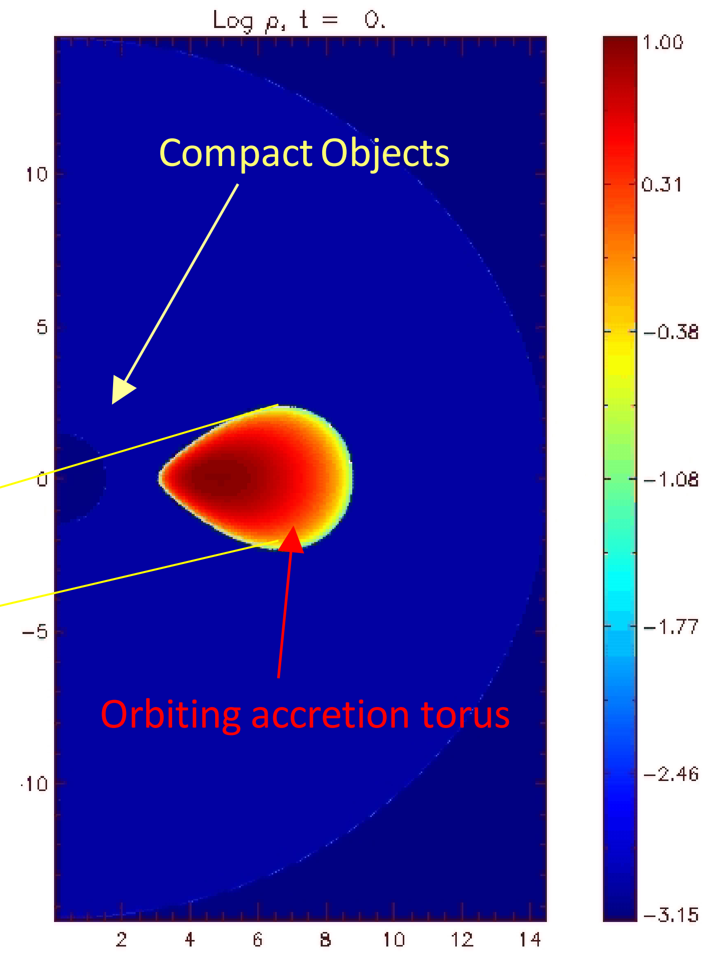

Accretion Disks: 3D local models

- Local approach based on ShearingBox models: based on a local expansion of the tidal forces in a reference frame corotating with the disk at some fiducial radius R_0. (shearing box approximation)
- allows to reach much higher resolutions[1]:

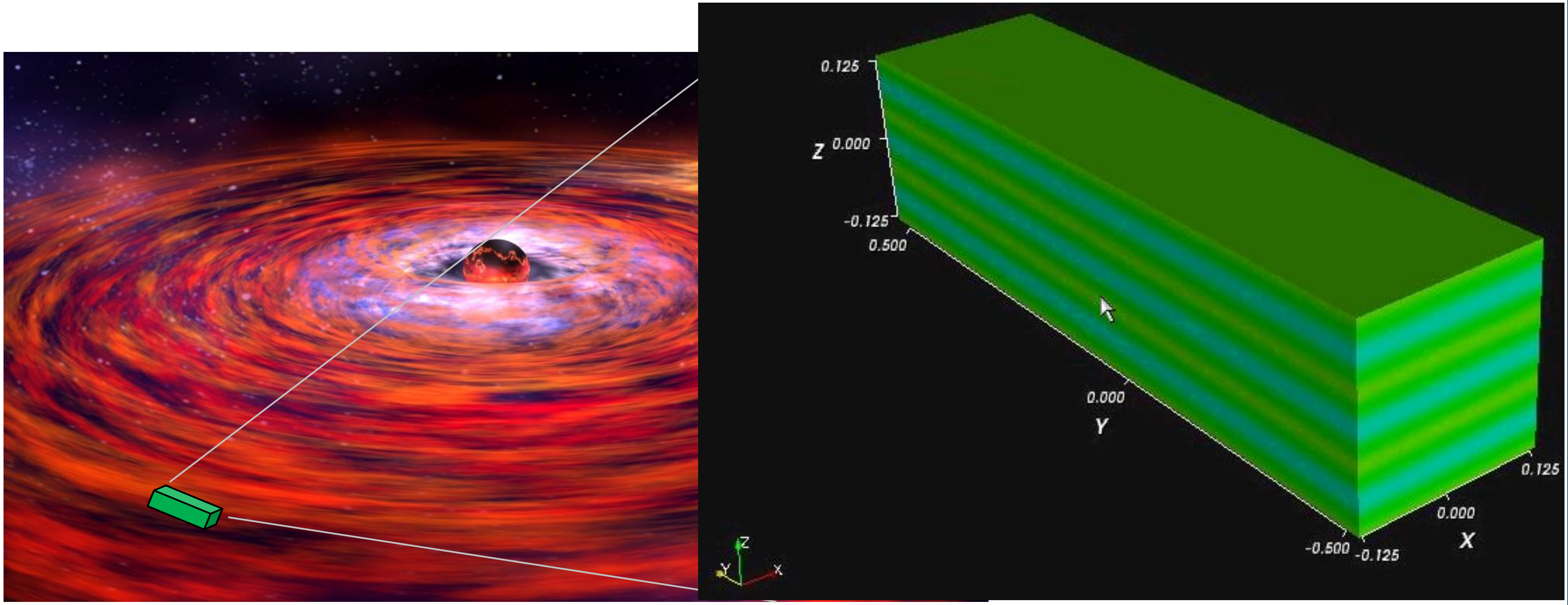

The Shearing Box Approximation

- Validity restricted to a small Cartesian box with a steady flow consisting of a linear shear velocity, normally considered as the basic flow.

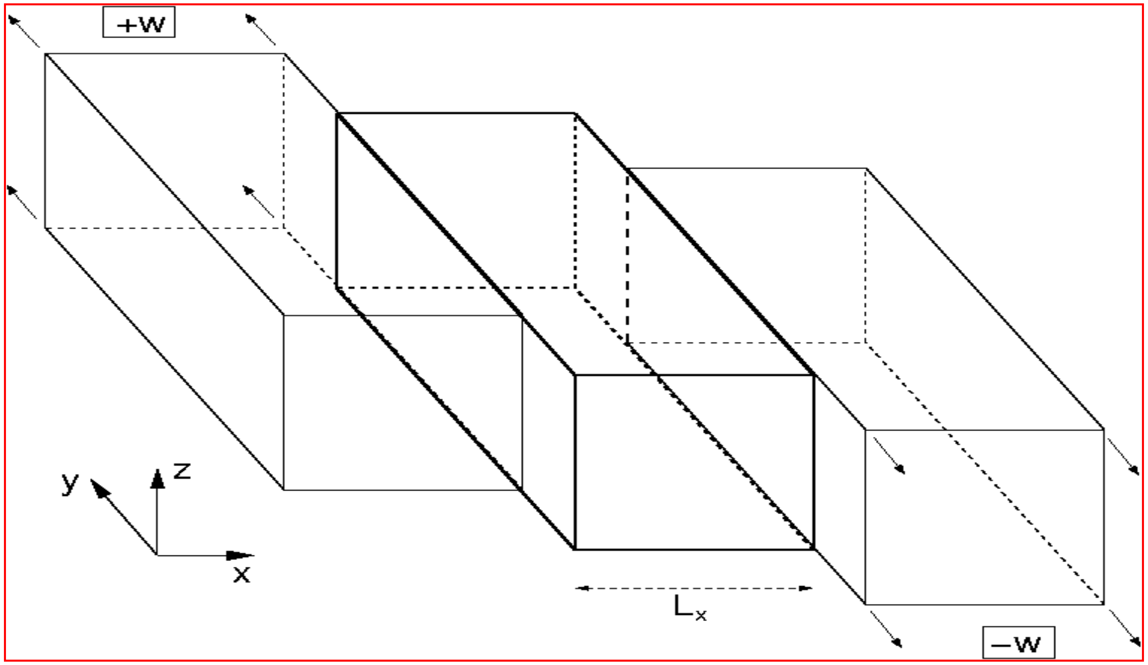

- While the computational box is periodic in the azimuthal (y) and vertical (z) directions, radial (x) boundary conditions are determined by “image” boxes sliding relative to the computational domain.

MRI: Channel Solution

- Simulations show intermittent behavior with episodes of efficient AM transport ("channel solutions")
- High correlation between components of magnetic field and velocity perturbations.
- Disruption by parasitic instabilities.
- However:
  - dominance of the channel seems peculiarity induced by an overly constrained geometry;
  - Increasing the aspect ratio, the system has more difficulty in forming the channel[1].

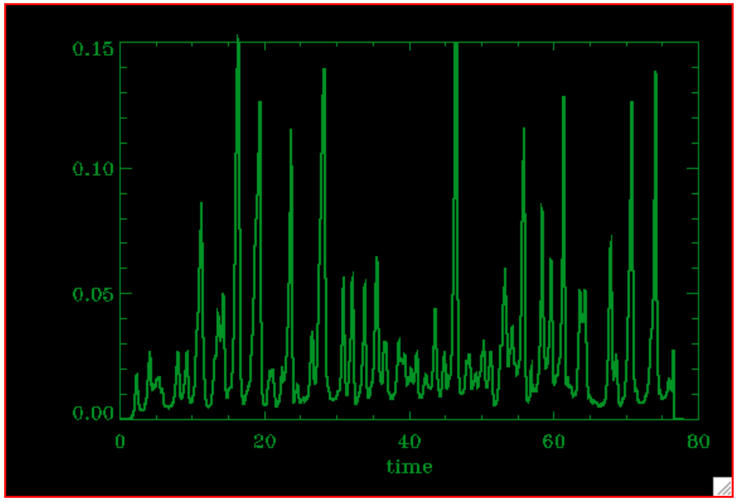

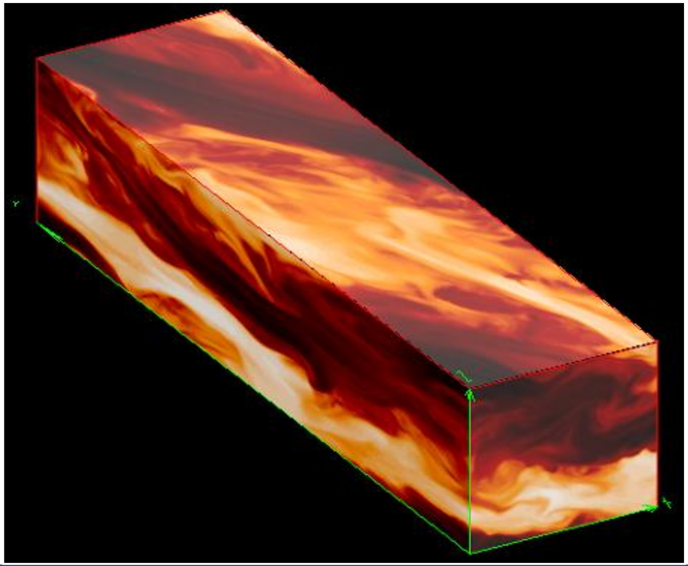

[1]Bodo et al., A&A(2008), 487,1B

Toward Global Simulations of Accretion Disks

- Shearing-box approximation probably unable to capture the physics of MRI in disks.

- Future simulations will tackle the full disk structure;

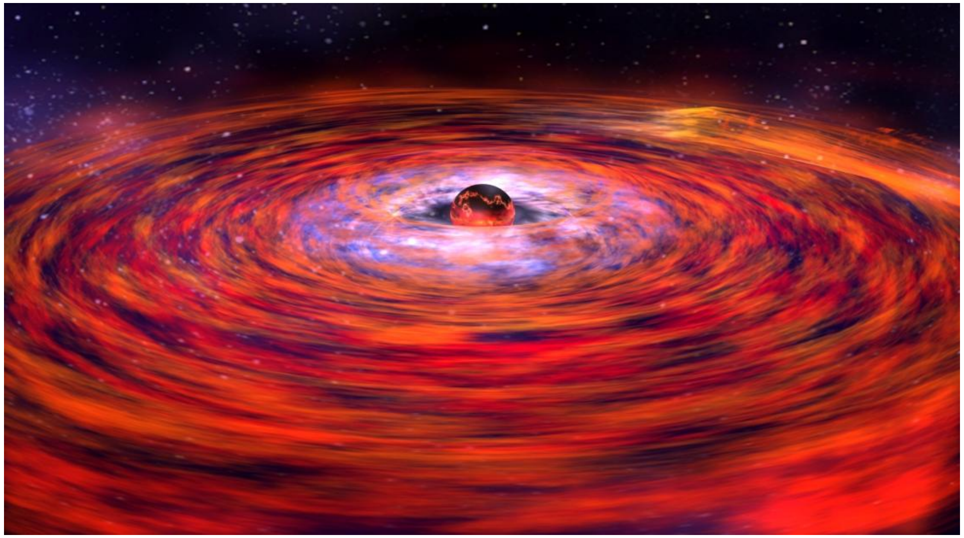

- Challenge: the scale disparity from global disk to the turbulent dissipative scale is enormous and inaccessible to computation;
- However: calculations with sufficient scale separation may give important answers → need for *very* high resolution (> 10^9 points, disk storage> 200 TB).

Stratified Simulations of Magnetized Disks

Turbulence and Accretion in 3D Global
MHD Simulations of Stratified Protoplanetary Disk

__Grid Resolution__: 384 x 192 x768
__Code__: PLUTO
__Author__: Flock et al, ApJ (2011) 735 122

3b. Astrophysical Applications: Relativistic Jets from AGN

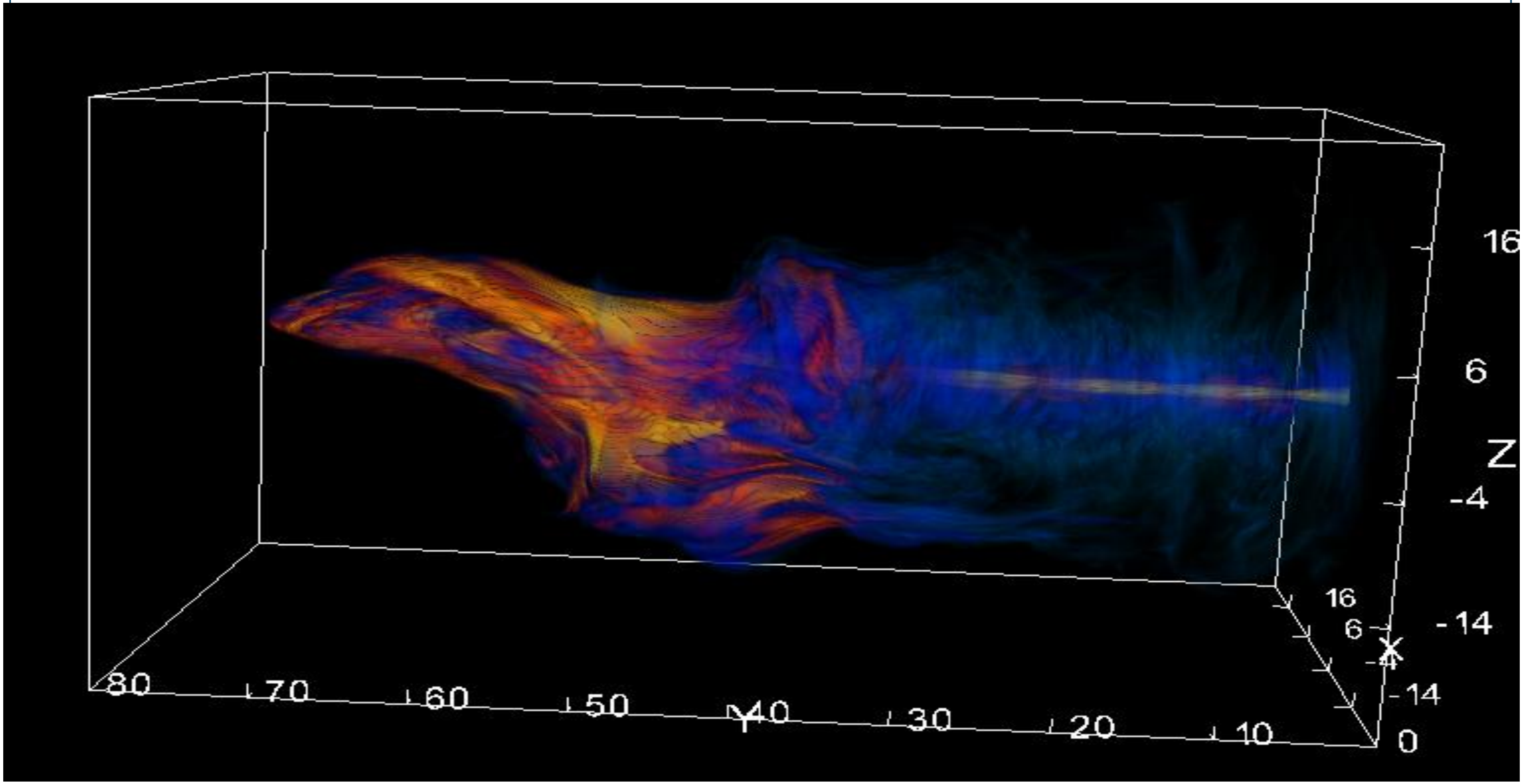

Extragalactic Jets: Morphology

- Supersonic, highly collimated plasma ejecta propagating away from the central engine
- Fundamental questions:
  - how can jet survive fluid instabilities ? Confinement ?
  - Morphology ⇔ physical properties (density, composition, magnetic fields…) ?
  - Jet emission mechanism ?
  - how do they decelerate ?
- Understanding the processes leading to momentum, energy and mass transfer to the environment is crucial and still largely unanswered.

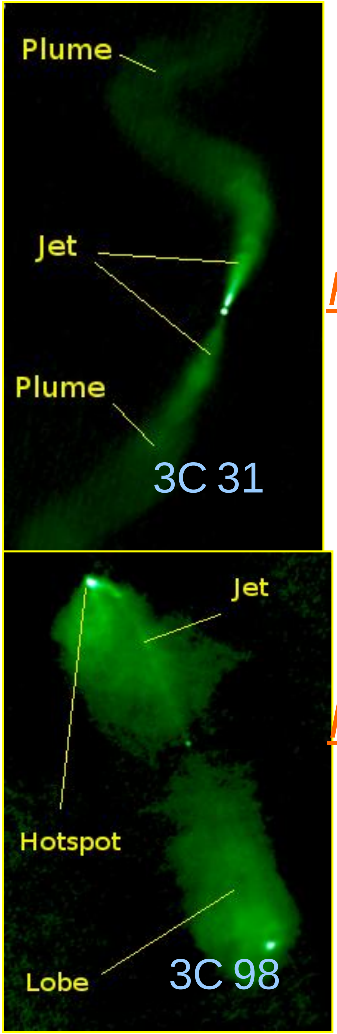

FR I

FR II

3D Simulations of Relativistic Jets

- 3D simulations by U. of Torino[1] (~ $2 \cdot 10^5$ CPU hours) confirm that the field topology is essential in determining the dynamics;

Poloidal (vertical) magnetic field:

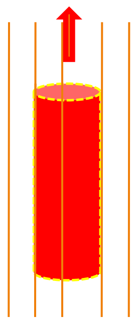

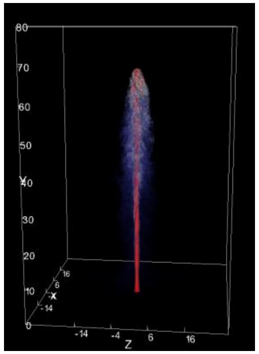

3D RMHD Jet

- Poloidal Field -

Grid Size:

640x1600x640

Simulation

10^5 Hours on

IBM Power 6

Cineca (Italy)

4 TB Data

Code:

PLUTO

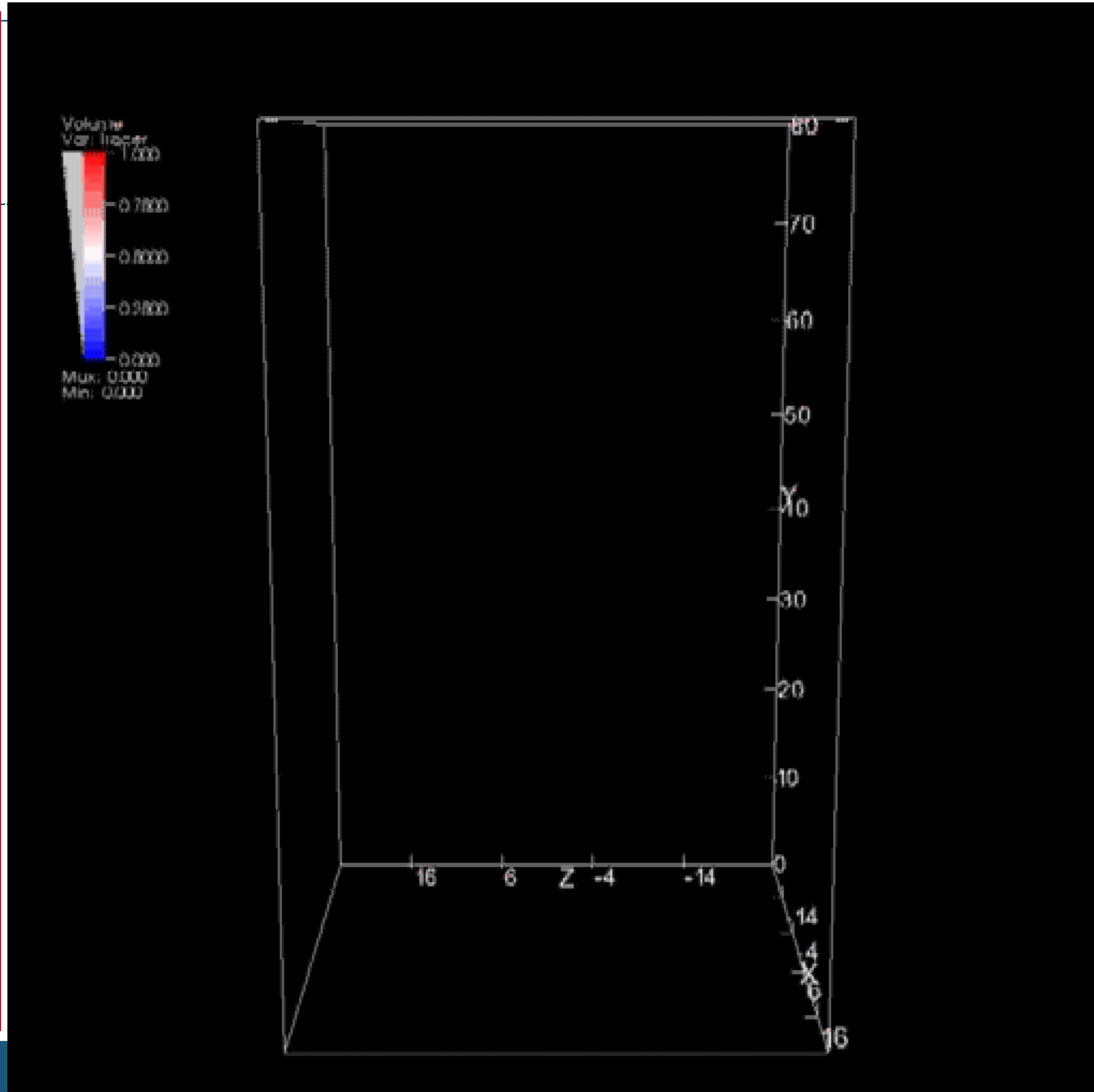

3D Simulations of Relativistic Jets

- 3D simulations by U. of Torino[1] (~ $2\cdot10^5$ CPU hours) confirm that the field topology is essential in determining the dynamics;

Poloidal (vertical) magnetic field:

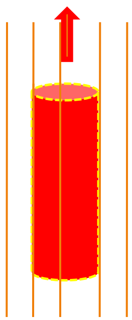

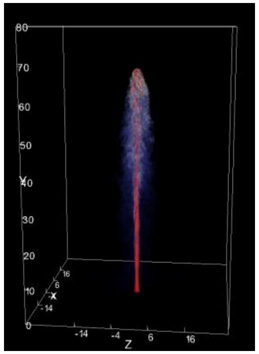

Toroidal (azimuthal) magnetic field

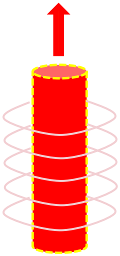

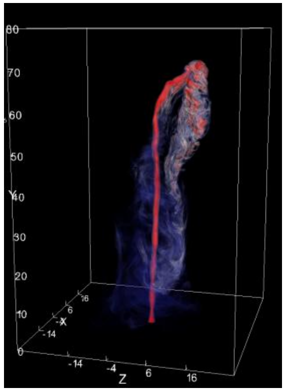

[1]Mignone et al. (MNRAS, 2009)

3D RMHD Jet
- Toroidal Field -

Grid Size:
640x1600x640

Simulation
10^5 Hours on
IBM Power 6
Cineca(Italy)
4 TB Data

Code:
PLUTO

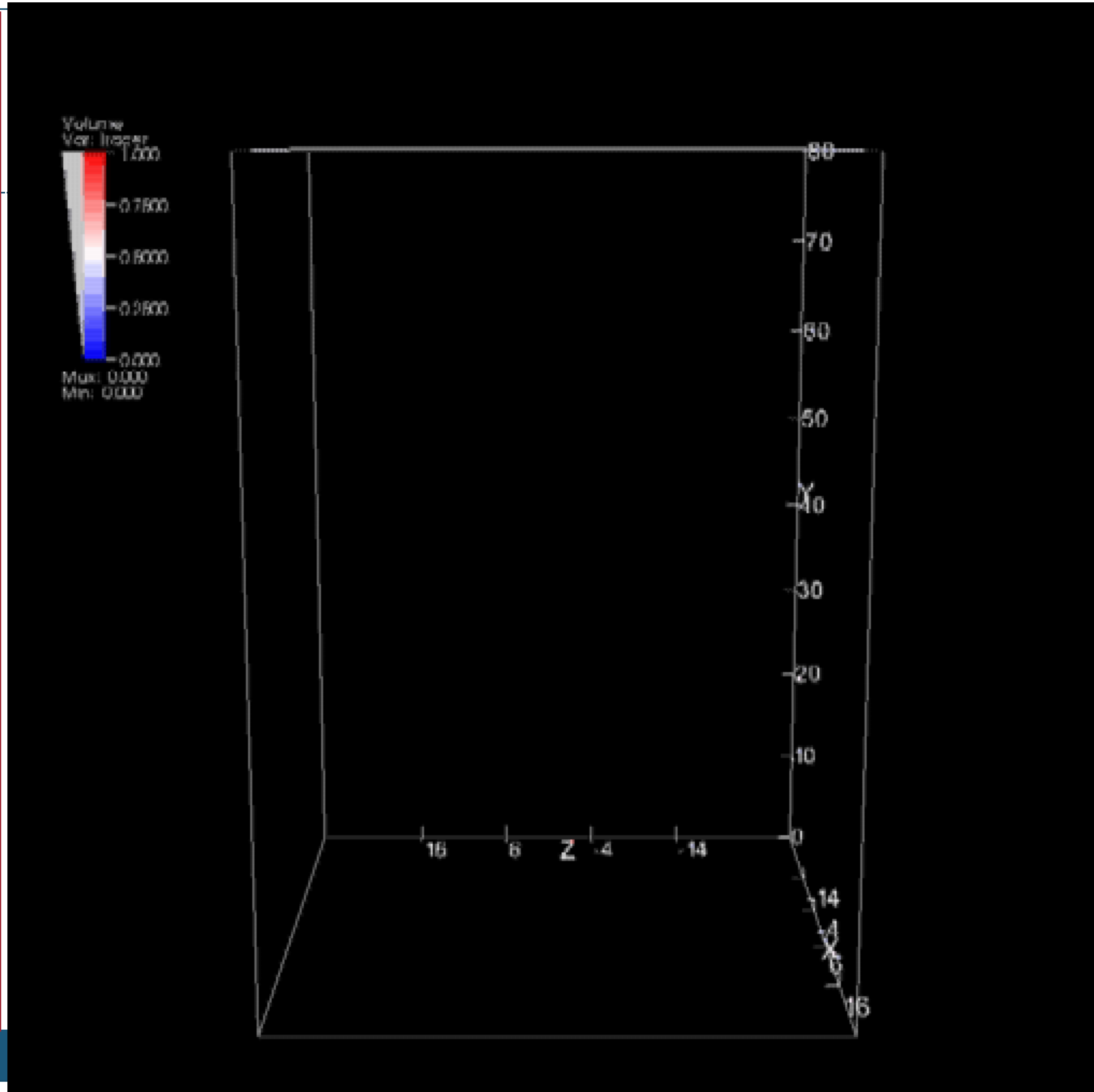

3D Simulations of Relativistic Jets

- 3D simulations by U. of Torino[1] (~ $2 \cdot 10^5$ CPU hours) confirm that the field topology is essential in determining the dynamics;

Poloidal (vertical) magnetic field:

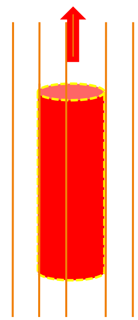

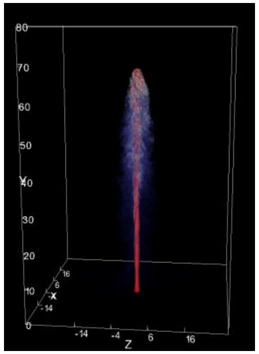

Toroidal (azimuthal) magnetic field

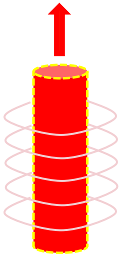

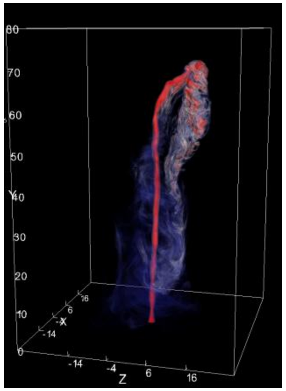

- Jet wiggling/beam deflection due to kink instabilities (m=1);
- → multiple sites where the jet impacts on the ambient forming shocks (compatible with multiple hotspots observed in several radiogalaxies);
- Backflow asymmetry replicates observational appearance of several objects.

[1]Mignone et al. (MNRAS, 2009)

Relativistic MHD jets: 2D vs 3D

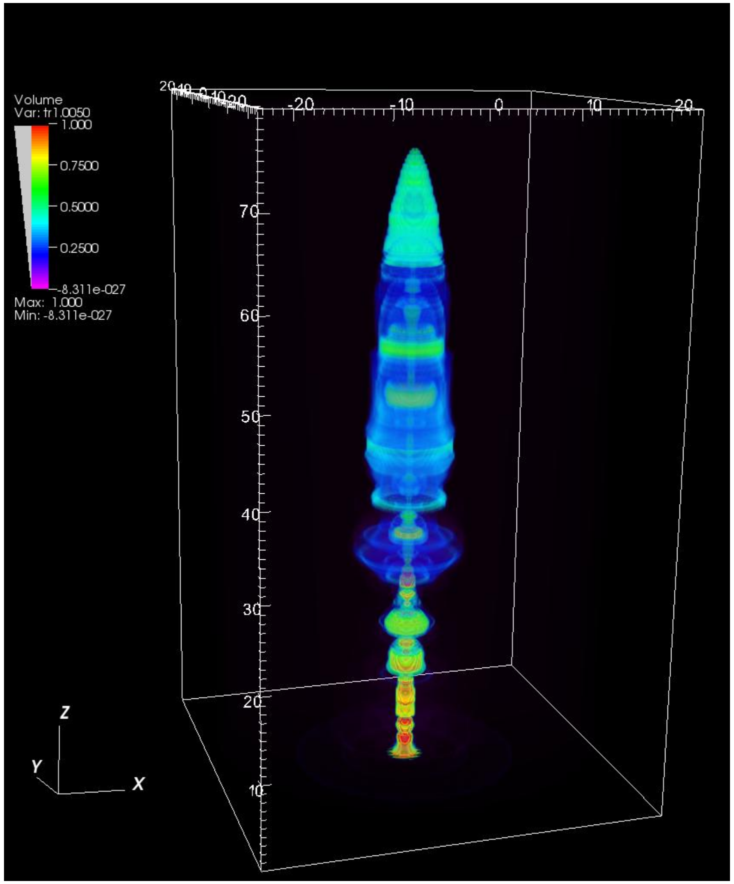

Axisym (“2.5” D)

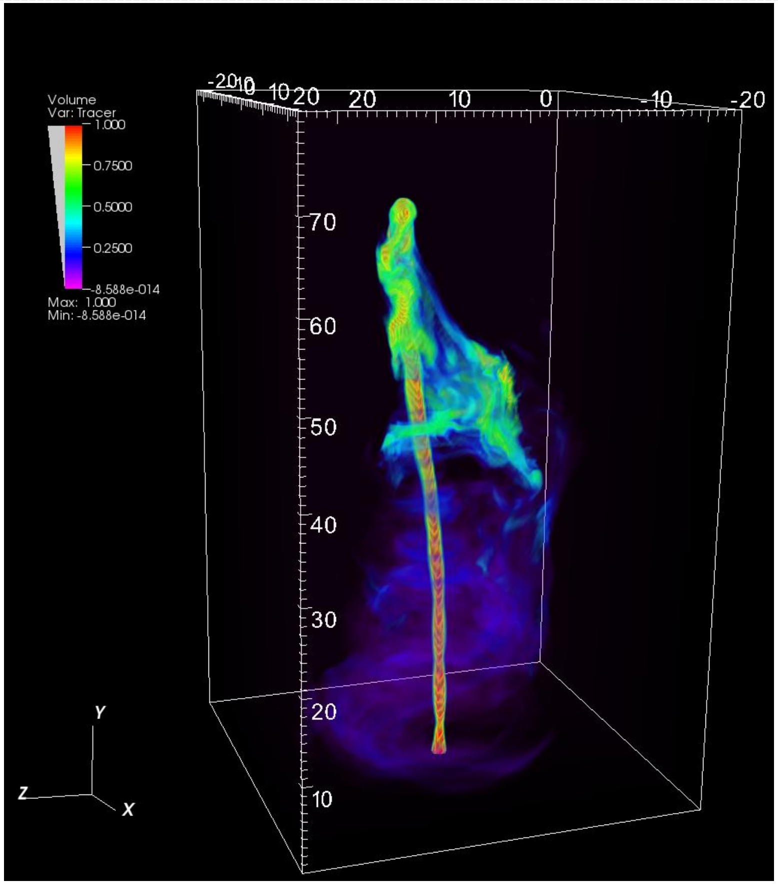

Fully 3-D

Pressure distribution

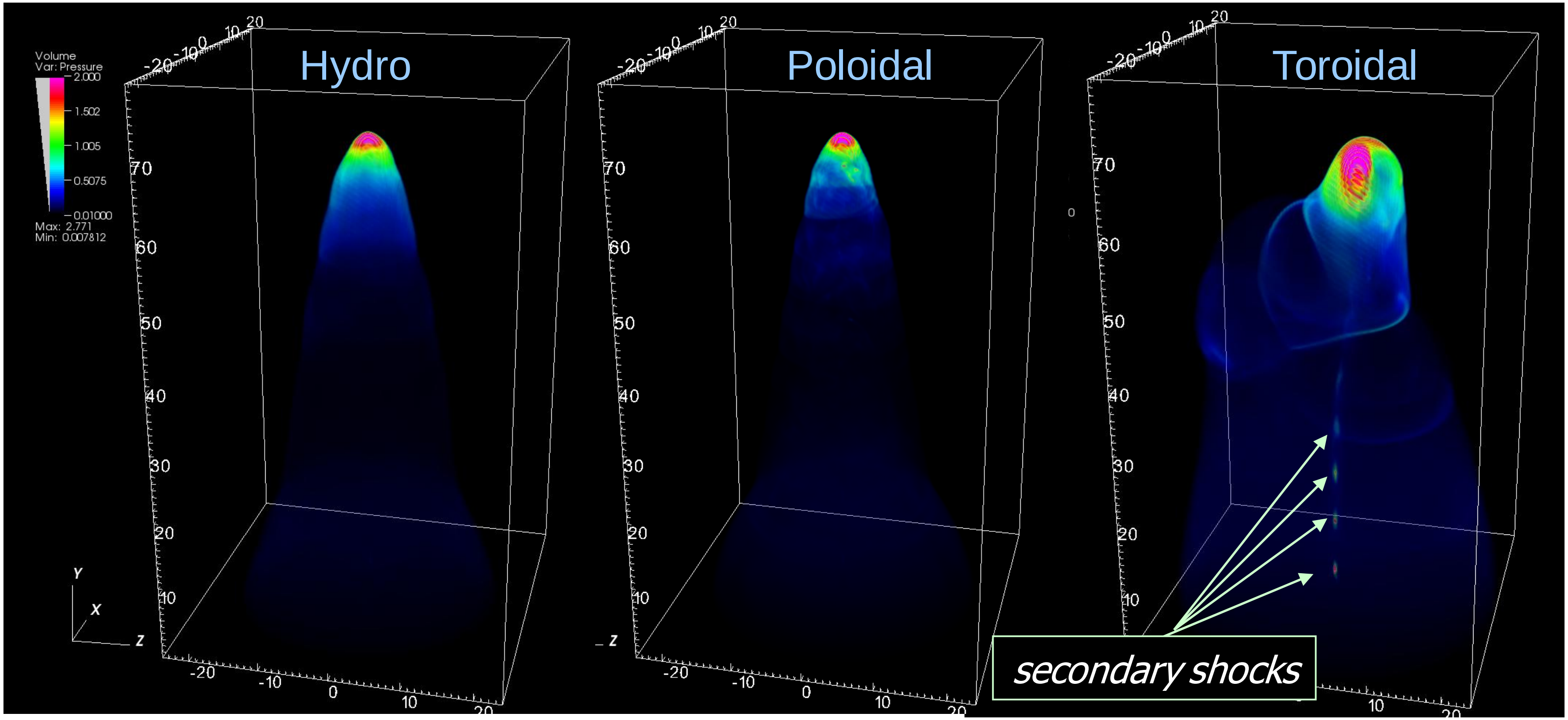

Simulation credits: The PLUTO Code

- PLUTO is modular parallel code providing a *multi-physics* as well as a *multi-algorithm* framework for the solution of conservation laws in astrophysics;

- Target: compressible, high-mach number flows with shocks in multiple spatial dimensions:
  - Compressible Euler / Navier Stokes equations;
  - Classical (ideal/resistive) Magnetohydrodynamics (MHD);
  - Special Relativistic hydro and MHD;
  - Heating/cooling processes, chemical network

- Variety of numerical methods:
  - Finite Volume / Finite Difference
  - Riemann solvers;
  - $2^{nd} – 5^{th}$ order interpolation techniques;

- Support static grid and Adaptive Mesh Refinement (AMR) computation

The PLUTO Code

- PLUTO is freely distributed at http://plutocode.ph.unito.it;
- More than 300 downloads in one year;

- References:
  - Mignone et al, Astrophys. J. Suppl. S. 170 (2007) 228. (static version)
  - Mignone et al, Astrophys. J. Suppl. S. 198 (2012) 7. (AMR version)

THE END

THANK YOU

FOR

YOUR ATTENTION